A neurotrophin functioning with a Toll regulates structural plasticity in a dopaminergic circuit

Jun Sun[1], Francisca Rojo-Cortés[1], Suzana Ulian-Benitez[1,2], Manuel G. Forero[3], Guiyi Li[1], Deepanshu Singh[1], Xiaocui Wang[1], Sebastian Cachero[4], Marta Moreira[1], Dean Kavanagh[5], Gregory Jefferis[4], Vincent Croset[6], and Alicia Hidalgo[1*]

1, Structural Plasticity & Regeneration Group, School of Biosciences, University of Birmingham, UK;

2, Current address: Buck Institute for Research on Aging, California, US;

3, Semillero Lún, Grupo D+Tec, Universidad de Ibagué, Colombia;

4, MRC LMB, Cambridge, UK;

5, Institute of Biomedical Research, University of Birmingham, UK.

6, Department of Biosciences, Durham University, UK.

*Author for correspondence:

00 44 (0)121 4145416

a.hidalgo@bham.ac.uk

Keywords: Drosophila, structural plasticity, cell survival, synaptogenesis, neurodegeneration, DNT-2, Toll-6, Kek-6, Toll-Like Receptor, Kekkon, Kek.

ABSTRACT

Experience shapes the brain, as neural circuits can be modified by neural stimulation or the lack of it. The molecular mechanisms underlying structural circuit plasticity and how plasticity modifies behaviour, are poorly understood. Subjective experience requires dopamine, a neuromodulator that assigns a value to stimuli, and it also controls behaviour, including locomotion, learning and memory. In *Drosophila*, Toll receptors are ideally placed to translate experience into structural brain change. *Toll-6* is expressed in dopaminergic neurons (DANs), raising the intriguing possibility that Toll-6 could regulate structural plasticity in dopaminergic circuits. *Drosophila* neurotrophin-2 (DNT-2) is the ligand for Toll-6, but whether it is required for circuit structural plasticity was unknown. Here, we show that *DNT-2* expressing neurons connect with DANs, and they modulate each other. Loss of function for *DNT-2* or its receptors *Toll-6* and kinase-less Trk-like *kek-6* caused DAN and synapse loss, impaired dendrite growth and connectivity, decreased synaptic sites and caused locomotion deficits. By contrast, over-expressed *DNT-2* increased dendrite complexity and promoted synaptogenesis. Neuronal activity increased synaptogenesis in DNT-2 and DANs, and over-expression of DNT-2 could mimic this effect. Altering the levels of DNT-2 or Toll-6 could also modify dopamine-dependent behaviours, including locomotion and long-term memory. We conclude that an activity-dependent feedback loop involving dopamine and DNT-2 labelled the circuits engaged, and DNT-2 with Toll-6 and Kek-6 induced structural plasticity in this circuit, modifying brain function.

INTRODUCTION

The brain can change throughout life, as new cells are formed or eliminated, axonal and dendritic arbours can grow or shrink, synapses can form or be eliminated[1-4]. Such changes can be driven by experience, that is, neuronal activity or the lack of it[1, 3-10]. Structural changes result in remodelling of connectivity patterns, and these bring about modifications of behaviour. These can be adaptive, dysfunctional or simply the consequence of opportunistic connections between neurons[11-13]. It is critical to understand how structural modifications to cells influence brain function. This requires linking with cellular resolution molecular mechanisms, neural circuits and resulting behaviours.

In the mammalian brain, the neurotrophins (NTs: BDNF, NGF, NT3, NT4) are growth factors underlying structural brain plasticity[14-16]. They promote neuronal survival, connectivity, neurite growth, synaptogenesis, synaptic plasticity and Long-Term Potentiation (LTP), via their Trk and $p75^{NTR}$ receptors[14-16]. In fact, all anti-depressants function by stimulating production of BDNF and signalling via its receptor TrkB, leading to increased brain plasticity[17, 18]. Importantly, NTs have dual functions and can also induce neuronal apoptosis, neurite loss, synapse retraction and Long-Term Depression (LTD), via $p75^{NTR}$ and Sortilin[15]. Remarkably, these latter functions are shared with neuroinflammation, which in mammals involves Toll-Like Receptors (TLRs)[19]. TLRs and Tolls have universal functions in innate immunity across the animals [20], and consistently with this, TLRs in the CNS are mostly studied in microglia. However, mammalian *TLRs* are expressed in all CNS cell types, where they can promote not only neuroinflammation, but also neurogenesis, neurite growth and synaptogenesis and regulate memory – independently of pathogens, cellular damage or disease[21-26]. Whether TLRs have functions in structural brain plasticity and behaviour remains little explored, and whether they can function together with neurotrophins in the mammalian brain is unknown.

Progress linking cellular and molecular events to circuit and behavioural modification has been rather daunting and limited using mammals[27]. The *Drosophila* adult brain is plastic and can be modified by experience and neuronal activity[28-36]. Different living conditions, stimulation with odorants or light, circadian rhythms, nutrition, long-term memory and experimentally activating or silencing neurons, modify

brain volume, alter circuit and neuronal shape, and remodel synapses, revealing experience-dependent structural plasticity[28, 31, 32, 34, 35, 37-42]. Furthermore, the *Drosophila* brain is also susceptible to neurodegeneration[43]. However, the molecular and circuit mechanisms underlying structural brain plasticity are mostly unknown in *Drosophila*.

Toll receptors are expressed across the Drosophila brain, in distinct but overlapping patterns that mark the anatomical brain domains[44]. Tolls share a common signalling pathway downstream, that can drive at least four distinct cellular outcomes – cell death, survival, quiescence, proliferation – depending on context[44-47]. They are also required for connectivity and structural synaptic plasticity and they can also induce cellular events independently of signalling[44, 46-50]. These nervous system functions occur in the absence of tissue damage or infection. This is consistent with the fact that - as well as universal functions in innate immunity - Tolls also have multiple non-immune functions also outside the CNS, including the original discovery of Toll in dorso-ventral patterning, cell intercalation, cell competition and others [45, 51-53]. The Toll distribution patterns in the adult brain and their ability to switch between distinct cellular outcomes means they are ideally placed to translate experience into structural brain change[44].

We had previously observed that in the adult brain, *Toll-6* is expressed in dopaminergic neurons[47]. Dopamine is a key neuromodulator that regulates wakefulness and motivation, experience valence, such as reward, and it is essential for locomotion, learning and memory[54-56]. In *Drosophila*, Dopaminergic neurons (DANs) form an associative neural circuit together with mushroom body Kenyon cells (KCs), Dorsal Anterior Lateral neurons (DAL) and Mushroom Body Output neurons (MBONs) [56-59]. Kenyon cells receive input from projection neurons of the sensory systems, they then project through the mushroom body lobes where they are intersected by DANs to regulate MBONs to drive behaviour [58, 60, 61]. This associative circuit is required for learning, long-term memory and goal-oriented behaviour [56, 59, 62]. During experience, involving sensory stimulation from the external world and from own actions, dopamine assigns a value to otherwise neutral stimuli, labelling the neural circuits engaged[58]. Thus, this raises the possibility that a link of Toll-6 to dopamine could enable translating experience into circuit modification to modulate behaviour.

In *Drosophila*, Toll receptors can function both independently of ligand-binding and by binding Spätzle (Spz) protein family ligands, also known as *Drosophila* neurotrophins (DNTs), that are sequence, structural and functional homologues of the mammalian NTs[46, 47, 63-68]. Like mammalian NTs, DNTs also promote cell survival, connectivity, synaptogenesis and structural synaptic plasticity, and they can also promote cell death, depending on context[46, 47, 49, 68, 69]. As well as Tolls, DNTs are also ligands for Kekkon (Kek) receptors, kinase-less homologues of the mammalian NT Trk receptors and are required for structural synaptic plasticity[49]. Importantly, the targets regulated by Tolls and Keks - ERK, NFκB, PI3K, JNK, CaMKII – are shared with those of mammalian NT receptors Trk and $p75^{NTR}$, and have key roles in structural and functional plasticity across the animals [13, 16, 46, 49, 53].

Here, we focus on Drosophila neurotrophin -2 (DNT-2), proved to be the ligand of Toll-6 and Kek-6, with in vitro, cell culture and in vivo evidence [46, 47, 49]. Here we asked how DNT-2, Toll-6 and Kek-6 are functionally related to dopamine, whether they and neuronal activity – as a proxy for experience - can modify neural circuits, and how structural circuit plasticity modifies dopamine-dependent behaviours.

RESULTS

DNT-2A, Toll-6 and Kek-6 neurons are integrated in a dopaminergic circuit

To allow morphological and functional analyses of *DNT-2* expressing neurons, we generated a *DNT-2Gal4* line using CRISPR/Cas9 and drove expression of the membrane-tethered-GFP *FlyBow1.1* reporter. We identified at least 12 DNT-2+ neurons and we focused on four anterior DNT-2A neurons per hemi-brain (Figure 1A). Using the post-synaptic marker Denmark, DNT-2A dendrites were found at the prow (PRW) and flange (FLA) region, whereas axonal terminals visualised with the pre-synaptic marker synapse defective 1 (Dsyd1-GFP) resided at the superior medial protocerebrum (SMP) (Figure 1B,D). We additionally found post-synaptic signal at the SMP and pre-synaptic signal at the FLA/PRW (Figure 1D), suggesting bidirectional communication at both sites. Using Multi-Colour Flip-Out (MCFO) to label individual cells stochastically[70, 71], single neuron clones revealed variability in the DNT-2A projections across individual flies (Figure 1C), consistently with developmental and activity-dependent structural plasticity in *Drosophila*[28, 32, 33, 35,

44, 72, 73]. We found that DNT-2A neurons are glutamatergic as they express the vesicular glutamate transporter vGlut (Figure 1E, left) and lack markers for other neurotransmitter types (Figure S1). DNT-2A terminals overlapped with those of dopaminergic neurons (Figure 1F), suggesting they could receive inputs from neuromodulatory neurons. In fact, single-cell RNA-seq revealed transcripts encoding the dopamine receptors *Dop1R1, Dop1R2, Dop2R* and/or *DopEcR* in DNT-2+ neurons[74]. Using reporters, we found that Dop2R is present in DNT-2A neurons, but not Dop1R2 (Figure 1E right, Figure S1C). Altogether, these data showed that DNT-2A neurons are excitatory glutamatergic neurons that could receive dopaminergic input both at PRW and SMP.

DNT-2 functions via Toll-6 and Kek-6 receptors, and *Toll-6* is expressed in DANs[47]. To identify the cells expressing *Toll-6* and *kek-6* and explore further their link to the dopaminergic system, we used *Toll-6Gal4[44]* and *kek-6Gal4*[49] to drive expression of membrane-tethered *FlyBbow1.1* and assessed their expression throughout the brain. Using anti-Tyrosine Hydroxilase (TH) - the enzyme that catalyses the penultimate step in dopamine synthesis - to visualise DANs, we found that Toll-6+ neurons included dopaminergic neurons from the PAMs, PPL1 and PPL2 clusters (Figure 1H, Figure S2D,F Table S1), whilst Kek-6+ neurons included PAM, PAL, PPL1, PPM2 and PPM3 dopaminergic clusters (Figure 1I, Figure S2B,E,F Table S1). DNT-2 can also bind various Tolls and Keks promiscuously[46, 47] and other *Tolls* are also expressed in the dopaminergic system: PAMs express multiple *Toll* receptors (Figure S2F) and all PPL1s express at least one *Toll* (Figure S2F). Using MCFO clones revealed that both *Toll-6* and *kek-6* are also expressed in Kenyon cells [44] (Figure S2I,J, Table S1), DAL neurons (Figure S2G,H, Table S1) and MBONs (Figure S2A-C). In summary, *Toll-6* and *kek-6* are expressed in DANs, DAL, Kenyon cells and MBONs (Figure 1G). These cells belong to a circuit required for associative learning, long-term memory and behavioural output, and DANs are also required for locomotion [54, 56, 59, 60, 75]. Altogether, our data showed that DNT-2A neurons are glutamatergic neurons that could receive dopamine as they contacted DANs and expressed the *Dop2R* receptor, and that in turn DANs expressed the DNT-2 receptors *Toll-6* and *kek-6*, and therefore could respond to DNT-2. These data suggested that there could be bidirectional connectivity between DNT-2A neurons and DANs, which we explored below.

Bidirectional connectivity between DNT-2A neurons and DANs

To verify the connectivity of DNT-2A neurons with DANs, we used various genetic tools. To identify DNT-2A output neurons, we used TransTango[76] (Figure 2A and Figure S3). DNT-2A RFP+ outputs included a subset of MB α'β' lobes, αβ Kenyon cells, tip of MB β'2, DAL neurons, dorsal fan-shaped body layer and possibly PAM or other dopaminergic neurons (Figure 2A, see Figure S3). Consistently, these DNT-2A output neurons express *Toll-6* and *kek-6* (Supplementary Table S1). To identify DNT-2A input neurons, we used BAcTrace[77]. This identified PAM-DAN inputs at SMP (Figure 2B). Altogether, these data showed that DNT-2A neurons receive dopaminergic neuromodulatory inputs, their outputs include MB Kenyon cells, DAL neurons and possibly DANs, and DNT-2 arborisations at SMP are bidirectional.

To further test the relationship between DNT-2A neurons and DANs, we reasoned that stimulating DANs would provoke either release or production of dopamine. So, we asked whether increasing DNT-2 levels in DNT-2 neurons could influence dopamine levels. For this, we over-express *DNT-2* in full-length form (i.e. *DNT-2FL*), as it enables to investigate non-autonomous functions of DNT-2 [49]. Importantly, DNT-2FL is spontaneously cleaved into the mature form[46, 47] (see discussion). Thus, we over-expressed *DNT-2FL* in DNT-2 neurons and asked whether this affected dopamine production, using mRNA levels for *TH* as readout. Using quantitative real-time PCR (qRT-PCR) we found that over-expressing *DNT2-FL* in DNT-2 neurons in adult flies increased *TH* mRNA levels in fly heads (Figure 2C). This showed that DNT-2 could stimulate dopamine production in neighbouring DANs.

Next, we wondered whether in turn DNT-2A neurons, that express *Dop2R*, could be modulated by dopamine. Binding of dopamine to D2-like Dop2R (also known as DD2R) inhibits adenylyl-cyclase, decreasing cAMP levels[78, 79]. Thus, we asked whether DNT-2A neurons received dopamine and signal via Dop2R. Genetic restrictions did not allow us to activate PAMs and test DNT-2 neurons, so we activated DNT-2 neurons and tested whether *Dop2R* knock-down would increase cAMP levels. We used the FRET-based cAMP sensor, Epac1-camps-50A[80]. When Epac1-camps-50A binds cAMP, FRET is lost, resulting in decreased YFP/CFP ratio over time. Indeed, *Dop2R* RNAi knock-down in DNT-2A neurons significantly

increased cAMP levels (Figure 2D), demonstrating that normally Dop2R inhibits cAMP signalling in DNT-2A cells. Importantly, this result meant that in controls, activating DNT-2A neurons caused dopamine release from DANs that then bound Dop2R to inhibit adenylyl-cyclase in DNT-2A neurons; this inhibition was prevented with *Dop2R* RNAi knock-down. Altogether, this shows that DNT-2 up-regulated TH levels (Figure 2E), whereas dopamine inhibited cAMP in DNT-2A neurons (Figure 2F).

In summary, DNT-2A neurons are connected to DANs, DAL and MB Kenyon cells, all of which express DNT-2 receptors *Toll-6* and *kek-6* and belong to a dopaminergic as well as associative learning and memory circuit. Furthermore, DNT-2A and PAM neurons form bidirectional connectivity. Finally, DNT-2 and dopamine regulate each other: DNT-2 increased dopamine levels (Figure 2E), and in turn dopamine via Dop2R inhibited cAMP signalling in DNT-2A neurons (Figure 2F). That is, an amplification was followed by negative feedback. This suggested that a dysregulation in this feedback loop could have consequences for dopamine-dependent behaviours and for circuit remodelling by the DNT-2 growth factor.

DNT-2 and Toll-6 maintain survival of PAM dopaminergic neurons in the adult brain

Above we showed that DNT-2 and PAM dopaminergic neurons are connected, so we next asked whether loss of function for *DNT-2* or *Toll-6* would affect PAMs. In wild-type flies, PAM-DAN number can vary between 220-250 cells per *Drosophila* brain, making them ideal to investigate changes in cell number[81]. Maintenance of neuronal survival is a manifestation of structural brain plasticity in mammals, where it depends on the activity-dependent release of the neurotrophin BDNF[15, 27]. Importantly, cell number can also change in the adult fly, as neuronal activity can induce neurogenesis via Toll-2, whereas DANs are lost in neurodegeneration models[44, 82]. Thus, we asked whether DNT-2 influences PAM-DAN number in the adult brain. We used *THGal4; R58E02Gal4* to visualise nuclear Histone-YFP in DANs (Figure 3A) and counted automatically YFP+ PAMs using purposely developed DeadEasy DAN software. $DNT2^{37}/DNT2^{18}$ mutant adult brains had fewer PAMs than controls (Figure 3B). Similarly, *Toll-6* RNAi knock-down in DANs also decreased PAM neuron number (Figure 3C). DAN loss was confirmed with anti-TH antibodies, as there were fewer TH+ PAMs in $DNT2^{37}/DNT2^{18}$ mutants (Figure 3D). Importantly, PAM cell loss was rescued by over-expressing

activated *Toll-6*^{CY} in DANs in *DNT-2* mutants (Figure 3D). Altogether, these data showed that DNT-2 functions via Toll-6 to maintain PAM neuron survival.

To ask whether DNT-2 could regulate dopaminergic neuron number specifically in the adult brain, we used *tubGal80*^{ts} to conditionally knock-down gene expression in the adult. PAMs were visualised with either *R58E02LexA>LexAop-nls-tdTomato* or *THGal4; R58E02Gal4 >histone-YFP* and counted automatically. Adult specific *DNT-2* RNAi knock-down decreased Tomato+ PAM cell number (Figure 3E). Similarly, RNAi *Toll-6* knock-down in DANs also decreased PAM neuron number (Figure 3F). Furthermore, knock-down of either *Toll-6* or *DNT-2* in the adult brain caused loss of PAM neurons visualised with anti-TH antibodies (Figure 3G). Cell loss was due to cell death, as adult specific *DNT-2 RNAi* knock-down increased the number of apoptotic cells labelled with anti-*Drosophila* Cleave caspase-1 (DCP-1) antibodies compared to controls (Figure 3H). This included Dcp-1+ PAMs (Figure 3H). By contrast, *DNT-2FL* over-expression in DNT2 neurons did not alter the incidence of apoptosis (Figure 3G), consistently with the fact that DNT-2FL spontaneously cleaves into the mature form[46, 47]. Thus, *DNT-2* and *Toll-6* knock-down specifically in the adult brain induced apoptosis and PAM-neuron loss.

Altogether, these data showed that sustained PAM neuron survival in development and in the adult brain depends on DNT-2 and Toll-6, and a reduction in their levels causes DAN cell loss, characteristic of neurodegeneration.

DNT-2 and its receptors are required for arborisations and synapse formation

We next asked whether DNT-2, Toll-6 and Kek-6 could influence dendritic and axonal arbours and synapses of dopaminergic neurons (Figure 4A). Visualising the pre-synaptic reporter Synaptotagmin-GFP (Syt-GFP) in PAM neurons, we found that *DNT-2*^{18}*/DNT-2*^{37} mutants completely lacked PAM synapses in the MB β,β' and γ lobes (Figure 4B). Interestingly, PAM connections at α,α' lobes were not affected (Figure 4B). This means that DNT-2 is required for synaptogenesis and connectivity of PAMs to MB β,β' and γ lobes.

PAM-β2β'2 neurons express *Toll-6* (Table S1) and their dendrites overlap axonal DNT2 projections. *Toll-6* RNAi knock-down in PAM -β2β'2 (with split-GAL4 *MB301BGal4* [57]), reduced dendrite complexity

(Figure 4C). To test whether DNT-2 could alter these dendrites, we over-expressed mature *DNT-2CK*. DNT-2CK is not secreted (from transfected S2 cells), but it is functional in vivo[46, 49, 68]. Importantly, over-expressed *DNT-2CK* functions cell-autonomously whereas *DNT-2FL* functions also non-autonomously, but they have similar effects[46, 49, 68]. Over-expression of *DNT-2CK* in PAM-β2β'2 increased dendrite arbour complexity (Figure 4D). Thus, DNT-2 and its receptor Toll-6 are required for dendrite growth and complexity in PAM neurons.

To ask whether DNT-2 could affect axonal terminals, we tested PPL1 axons. PPL1-γ1-pedc neurons have a key function in long-term memory[57, 58, 83, 84] and express both *Toll-6* and *kek-6* (Table S1). Using split-GAL4 line M*B320C-Gal4* to visualise PPL1 axonal arbours, RNAi knock-down of either *Toll-6*, *kek-6* or both together caused axonal misrouting away from the mushroom body peduncle (Figure 4E,E', Chi Square $p<0.05$, see Table S2). Similarly, *DNT-2FL* over-expression also caused PPL1 misrouting (Figure 4F, Chi-Square $p<0.05$, see Table S2). Thus, DNT-2, Toll-6 and Kek-6 are required for appropriate targeting and connectivity of PPL1 DAN axons.

To test whether this signalling system was required specifically in the adult brain, we used *tubGAL80^{ts}* to knock-down *Toll-6* and *kek-6* with RNAi conditionally in the adult and visualised the effect on synaptogenesis using the post-synaptic reporter Homer-GCaMP and anti-GFP antibodies. Adult-specific *Toll-6 kek-6* RNAi knock-down in PAM neurons did not affect synapse number (not shown), but it decreased post-synaptic density size, both at the MB lobe and at the SMP dendrite (Figure 4G). These data meant that the DNT-2 receptors *Toll-6* and *kek-6* continue to be required in the adult brain for appropriate synaptogenesis.

Altogether, these data showed that DNT-2, Toll-6 and Kek-6 are required for dendrite branching, axonal targeting and synapse formation. The shared phenotypes from altering the levels of *DNT-2* and *Toll-6 kek-6* in arborisations and synapse formation, support their joint function in these contexts. Importantly, these findings showed that connectivity of PAM and PPL1 dopaminergic neurons depend on DNT-2, Toll-6 and Kek-6.

DNT-2 neuron activation and *DNT-2* over-expression induced synapse formation in target PAM dopaminergic neurons

The above data showed that DNT-2, Toll-6 and Kek-6 are required for DAN cell survival, arborisations and synaptogenesis in development and adults. This meant that the dopaminergic circuit remains plastic in adult flies. Thus, we wondered whether neuronal activity could also induce remodelling in PAM neurons. In mammals, neuronal activity induces translation, release and cleavage of BDNF, and BDNF drives synaptogenesis[14, 15, 27, 85]. Thus, we first asked whether neuronal activity could influence DNT-2 levels or function. We visualised tagged DNT-2FL-GFP in adult brains, activated DNT-2 neurons with TrpA1 at 30°C, and found that DNT-2 neuron activation increased the number of DNT-2-GFP vesicles produced (Supplementary Figure S4A). Furthermore, neuronal activity also facilitated cleavage of DNT-2 into its mature form. In western blots from brains over-expressing *DNT-2FL-GFP*, the levels of full-length DNT-2FL-GFP were reduced following neuronal activation and the cleaved DNT-2CK-GFP form was most abundant (Supplementary Figure S4B). These findings meant that, like mammalian BDNF, also DNT-2 can be influenced by activity.

Thus, we asked whether neuronal activity and DNT-2 could influence synapse formation. We first tested DNT-2 neurons. Activating DNT-2 neurons altered DNT-2 axonal arbours (Figure 5A) and it increased Homer-GFP+ synapse number in the DNT-2 SMP arbour (Figure 5B and Figure S5). Next, as DNT-2 and PAMs form bidirectional connexions at SMP (Figure 1, 2), we asked whether activating DNT-2 neurons could affect target PAM neurons. To manipulate DNT-2 neurons and visualise PAM neurons concomitantly, we combined *DNT-2GAL4* with the *PAM-LexAOP* driver. However, there were no available *LexA/OP* post-synaptic reporters, so we used the pre-synaptic *LexAOP-Syt-GCaM*P reporter instead, which labels Synaptotagmin (Syt), and GFP antibodies. Activating DNT-2 neurons with TrpA1 increased the number of Syt+ synapses at the PAM SMP arbour (Figure 5C) and reduced their size (Figure 5C). This was consistent with the increase in Homer-GFP+ PSD number in stimulated DNT-2 neurons (Figure 5B). Neuronal activity can induce ghost boutons, immature synapses that are later eliminated [86]. Here, the coincidence of increased pre-synaptic Syt-GFP from PAMs and post-synaptic Homer-GFP from DNT-2 neurons at SMP

revealed that newly formed synapses were stable. PAM neurons also send an arborisation at the MB β, β', γ lobes, but DNT-2 neuron activation did not affect synapse number nor size there (Figure 5C). These data showed that activating DNT-2 neurons induced synapse formation at the SMP connection with PAMs.

Finally, we asked whether, like activity, DNT-2FL could also drive synaptogenesis. We over-expressed *DNT-2FL* in DNT-2 neurons and visualised the effect in PAM neurons. Over-expression of *DNT-2FL* in DNT-2 neurons did not alter Syt+ synapse number at the PAM SMP dendrite, but it increased bouton size (Figure 5D). By contrast, at the MB β, β' lobe arborisation, over-expressed *DNT-2* did not affect Syt+ bouton size, but it increased the number of output synapses (Figure 5D). This data showed that DNT-2 released from DNT-2 neurons could induce synapse formation in PAM target neurons.

Altogether, these data showed that neuronal activity induced synapse formation, it stimulated production and cleavage of DNT-2, and DNT-2 could induce synapse formation in target neurons.

Structural plasticity by DNT2 modified dopamine-dependent behaviour

Circuit structural plasticity raises the important question of what effect it could have on brain function, i.e. behaviour. Data above showed that DANs and DNT-2 neurons are functionally connected, that loss of function for *DNT-2* or its receptors caused dopaminergic neuron loss, altered DAN arborisations and caused synapse loss or reduction in size, and that DNT-2 could induce dendrite branching and synaptogenesis, altogether modifying circuit connectivity. To measure the effect of such circuit modifications on brain function, we used dopamine-dependent behaviours as readout.

Startle-induced negative geotaxis (also known as the climbing assay) is commonly used as a measure of locomotor ability and requires dopamine and specifically PAM neuron function[87, 88]. We tested the effect of *DNT-2* or *Toll-6* and *kek-6* loss of function in climbing, and both *DNT-2*^{37}/*DNT-2*^{18} mutants and flies in which *DNT-2* was knocked-down in DNT-2 neurons in the adult stage had lower climbing ability than controls (Figure 6A). Similarly, when *Toll-6* and *kek-6* were knocked-down with RNAi in the adult using a *Toll-6-* or a *PAM-GAL4* neuron driver, climbing was also reduced (Figure 6B). Importantly,

over-expressing activated *Toll-6*^{CY} in DANs rescued the locomotion deficits of *DNT-2* mutants, showing that DNT-2 functions via Toll-6 in this context (Figure 6C).

We also tracked freely moving flies in an open arena[89]. Interestingly, in that setting, locomotion of homozygous *DNT-2*^{37}*/DNT-2*^{18} mutants was similar to that of controls, but over-expression of *Toll-6*^{CY} in their DANs increased locomotion as flies walked longer distances and spent less time immobile (Figure 6D). Adult flies over-expressing *DNT2-FL* walked faster (Figure 6E and Figure S5) and so did those where DNT-2 neurons were activated with TrpA1 (Figure 6F and Figure S6), consistently with the fact that neuronal activity increased DNT-2 production (Figure S4A) and that DNT-2FL increased TH levels (Figure 2C). Therefore, increased Toll-6^{CY} levels in DANs increase locomotion and increased DNT-2 levels are sufficient to boost walking speed. Interestingly, both loss and gain of function for *DNT-2* also caused seizures (Figure S7). Thus, dopamine-dependent locomotion is regulated by the function of DNT-2, Toll-6 and Kek-6.

Next, as dopamine is an essential neurotransmitter for learning and memory[56], we asked whether DNT-2 might influence appetitive olfactory conditioning. Starved flies were trained to associate a sugar reward with an odour (CS+) while another odour was presented without sugar (CS-), and their preference for CS+ versus CS- was measured, 24h after training (as in [90, 91]). Remarkably, over-expression of *DNT-2FL* in DNT-2 neurons in adults enhanced appetitive long-term memory (Figure 6G), consistent with the positive role of DNT-2 in synaptogenesis that we demonstrated above.

In summary, we have shown that alterations in DNT-2, Toll-6 and Kek-6 levels that caused structural phenotypes in DANs also modified dopamine-dependent behaviours, locomotion and long-term memory.

DISCUSSION

Our findings indicate that structural plasticity and degeneration in the brain are two manifestations of a shared molecular mechanism that could be modulated by experience. Loss of function for *DNT-2, Toll-6* and *kek-6* caused cell loss, affected arborisations and synaptogenesis in DANs and impaired locomotion; neuronal activity increased DNT-2 production and cleavage and remodelled connecting DNT-2 and PAM

synapses; and over-expression of *DNT-2* increased TH levels, PAM dendrite complexity, and synaptogenesis, and it enhanced locomotion and long-term memory.

It was remarkable to find that dopaminergic neurons in the *Drosophila* adult brain require sustained trophic support, and this is functionally relevant as it can influence behaviour. Loss of *DNT-2* function in mutants, constant loss of *Toll-6* function in DANS and adult-restricted knock-down of either *DNT-2* (in DNT-2 neurons) or *Toll-6* (in Toll-6 neurons and in DANs) all resulted in DAN cell loss, verified with three distinct reporters, and consistently with the increase in DAN apoptosis. Furthermore, DAN cell loss in *DNT-2* mutants could be rescued by the over-expression of *Toll-6* in DANs. These findings are reminiscent of the increased apoptosis and cell loss in adult brains with *Toll-2* loss of function[44], and the support of DAN survival by Toll-1 and Toll-7 driven autophagy[92]. They are also consistent with a report that loss of function for *DNT-2* or *Toll-6* induced apoptosis in the third instar larval optic lobes[93]. This did not result in neuronal loss - which was interpreted as due to Toll-6 functions exclusive to glia [93] - but instead of testing the optic lobes, neurons of the larval abdominal ventral nerve cord (VNC) were monitored[93]. In the VNC, Toll-6 and -7 function redundantly and knock-down of both is required to cause neuronal loss in embryos[47], whereas in L3 larvae and pupae the phenotype is compounded by their pro-apoptotic functions[46]. It is crucial to consider that the DNT-Toll signalling system can have distinct cellular outcomes depending on context, cell type and time, ie stage [44, 46, 94]. Our work shows that in the adult *Drosophila* brain DAN neurons receive secreted growth factors that maintain cellular integrity, and this impacts behaviour. Consistently with our findings, *Drosophila* models of Parkinson's Disease reproduce the loss of DANs and locomotion impairment of human patients[54, 82, 87, 88]. Dopamine is required for locomotion, associative reward learning and long-term memory[54-56, 58, 87, 88]. In *Drosophila*, this requires PAM, PPL1 and DAL neurons and their connections to Kenyon Cells and MBONs[56, 58-61]. DNT-2 neurons are connected to all these neuron types, which express *Toll-6* and *kek-6,* and modifying their levels affected locomotion and long-term memory. Altogether, our data demonstrate that structural changes caused by altering DNT-2, Toll-6 and Kek-6 modified dopamine-dependent behaviours, providing a direct link between molecules, structural circuit plasticity and behaviour.

We used neuronal activation as a proxy for experience, but the implication is that experience would similarly drive the structural modification of circuits labelled by neuromodulators. Similar manipulations of activity have previously revealed structural circuit modifications. For example, hyperpolarising olfactory projection neurons increased microglomeruli number, active zone density and post-synaptic site size in the calyx, whereas inhibition of synaptic vesicle release decreased the number of microglomeruli and active zones[32]. There is also evidence that experience can modify circuits and behaviour in *Drosophila.* For example, natural exposure to light and dark cycles maintains the structural homeostasis of presynaptic sites in photoreceptor neurons, which breaks down in sustained exposure to light[35]. Prolonged odour exposure causes structural reduction at the antennal lobe and at the output pre-synaptic sites in the calyx, and habituation [37, 95]. Similarly, prolonged exposure to CO2 caused a reduction in output responses at the lateral horn and habituation[34]. Our findings are also consistent with previous reports of structural plasticity during learning in *Drosophila.* Hypocaloric food promotes structural plasticity in DANs, causing a reduction specifically in connections between DANs and Kenyon cells involved in aversive learning, thus decreasing the memory of the aversive experience[31]. By contrast, after olfactory conditioning, appetitive long-term memory increased axonal collaterals in projection neurons, and synapse number at Kenyon cell inputs in the calyx[28]. Our data provide a direct link between a molecular mechanism, synapse formation in a dopaminergic circuit and behavioural performance. Since behaviour is a source of experience, the discovery that a neurotrophin can function with a Toll and a neuromodulator to sculpt circuits provides a mechanistic basis for how experience can shape the brain throughout life.

Importantly, in humans structural brain plasticity (e.g. adult neurogenesis, neuronal survival, neurite growth and synaptogenesis) correlates with anti-depressant treatment, learning, physical exercise and well-being[7, 10, 18, 96]. Conversely, neurite, synapse and cell loss, correlate with ageing, neuroinflammation, psychiatric and neurodegenerative conditions[3, 27, 85, 97-99]. Understanding how experience drives the switch between generative and destructive cellular processes shaping the brain is critical to understand brain function, in health and disease. In this context, the mechanism we have discovered could also operate in the human brain. In fact, there is deep evolutionary conservation in DNT-2

vs mammalian NT function (eg BDNF), but some details differ. Like mammalian NTs, full-length DNTs/Spz proteins contain a signal peptide, an unstructured pro-domain and an evolutionarily conserved cystine-knot of the NT family[46, 68, 100]. Cleavage of the pro-domain releases the mature cystine-knot (CK). In mammals, full-length NTs have opposite functions to their cleaved forms (e.g. apoptosis vs cell survival, respectively). However, DNT-2FL is cleaved by intracellular furins, and although DNT-2 can be found both in full-length or cleaved forms in vivo, it is most abundantly found cleaved[46, 47, 68]. As a result, over-expressed *DNT-2FL* does not induce apoptosis and instead it promotes cell survival[46]. The same functions are played by over-expressed mature *DNT-2CK* as by *DNT-2FL*[46, 49, 68]. In S2 cells, transfected DNT-2CK is not secreted, but when over-expressed in vivo it is functional [46, 49, 68] (and this work). In fact, over-expressed *DNT-2CK* also maintains neuronal survival, connectivity and synaptogenesis[46, 49, 68] (and this work). Similarly, over-expressed mature *spz-1-C106* can rescue the *spz-1*-null mutant phenotype[101] and over-expressed *DNT-1CK* can promote neuronal survival, connectivity and rescue the *DNT-1* mutant phenotype[68]. Consistently, both DNT-2FL and DNT-2CK have neuro-protective functions promoting cell survival, neurite growth and synaptogenesis[46, 49, 68, 69] (and this work). Importantly, over-expressing *DNT-2FL* enables to investigate non-autonomous functions of DNT-2[49]. We have shown that *DNT-2FL* can induce synaptogenesis non-autonomously in target neurons. Similarly, DNT-2 is a retrograde factor at the larval NMJ, where transcripts are located post-synaptically in the muscle, DNT-2FL-GFP is taken up from muscle by motorneurons, where it induces synaptogenesis[49, 69]. Importantly, we have shown that neuronal activity increased production of tagged DNT-2-GFP, and its cleavage. In mammals, neuronal activity induces synthesis, release and cleavage of BDNF, leading to neuronal survival, dendrite growth and branching, synaptogenesis and synaptic plasticity (ie LTP)[14, 15, 27, 102, 103]. Like BDNF, DNT-2 also induced synaptogenesis and increased bouton size. It may not always be possible to disentangle primary from compensatory phenotypes, as Hebbian, homeostatic and heterosynaptic plasticity can concur[99, 104]. Mammalian BDNF increases synapse number, spine size and long-term potentiation (LTP), but it can also regulate homeostatic plasticity and long-term depression (LTD), depending on timing, levels and site of action[14, 15, 27]. In this context, neuronal stimulation of DNT-2 neurons induced synapse formation in

PAM neuron SMP dendrites, whereas DNT-2 over-expression from DNT-2 neurons increased synapse size at SMP and synapse number in PAM outputs at the mushroom body lobes. These distinct effects could be due to the combination of plasticity mechanisms and range of action. Neuronal activity can induce localised protein synthesis that facilitates local synaptogenesis and stabilises emerging synapses[99]. By contrast, DNT-2 induced signalling via the nucleus can facilitate synaptogenesis at longer distances, in output sites. In any case, synaptic remodelling is the result of concurring forms of activity-dependent plasticity altogether leading to modification in connectivity patterns[99, 104]. Long-term memory requires synaptogenesis, and in mammals this depends on BDNF, and its role in the protein-synthesis dependent phase of LTP[14, 27, 105]. BDNF localised translation, expression and release are induced to enable long-term memory[14, 27, 105, 106]. We have shown that similarly, over-expressed *DNT-2FL* increased both synaptogenesis in sites involved in reward learning, and long-term memory after appetitive conditioning.

The relationship of NTs with dopamine is also conserved. DNT-2 and DAN neurons form bidirectional connectivity that modulates both DNT-2 and dopamine levels. Similarly, mammalian NTs also promote dopamine release and the expression of DA receptors[107, 108]. Furthermore, DAN cell survival is maintained by DNT-2 in *Drosophila,* and similarly DAN cell survival is also maintained by NT signalling in mammals and fish[109, 110]. Importantly, we showed that activating DNT-2 neurons increased the levels and cleavage of DNT-2, up-regulated DNT-2 increased *TH* expression, and this initial amplification resulted in the inhibition of cAMP signalling by dopamine via Dop2R in DNT-2 neurons. This negative feedback could drive a homeostatic reset of both DNT-2 and dopamine levels, important for normal brain function. In fact, alterations in DNT-2 levels could cause seizures. Importantly, alterations in both NTs and dopamine underlie many psychiatric disorders and neurodegenerative diseases in humans[27, 99, 108, 110, 111].

We have uncovered a novel mechanism of structural brain plasticity, involving a NT ligand functioning via a Toll and a kinase-less Trk-family receptor in the adult *Drosophila* brain. Toll receptors in the CNS can function via ligand dependent and ligand-independent mechanisms[45]. However, in the context analysed, Toll-6 and Kek-6 function in structural circuit plasticity depends on their ligand DNT-2. This is also consistent with their functions promoting axonal arbour growth, branching and synaptogenesis

at the NMJ[49]. Furthermore, Toll-2 is also neuro-protective in the adult fly brain, and loss of *Toll-2* function caused neurodegeneration and impaired behaviour [44]. There are six *spz/DNT*, nine *Toll* and six *kek* paralogous genes in *Drosophila*[49, 112-114], and at least seven *Tolls* and three adaptors are expressed in distinct but overlapping patterns in the brain [44]. Such combinatorial complexity opens the possibility for a fine-tuned regulation of structural circuit plasticity and homeostasis in the brain.

Drosophila and mammalian NTs may have evolved to use different receptor types to elicit equivalent cellular outcomes. In fact, in mammals, NTs function via Trk, $p75^{NTR}$ and Sortilin receptors, to activate ERK, PI3K, NFκB, JNK and CaMKII[15, 27]. Similarly, DNTs with Tolls and Keks also activate ERK, NFκB, JNK and CaMKII in the *Drosophila* CNS[45-47, 49]. However, alternatively, NTs may also use further receptors in mammals. Trks have many kinase-less isoforms, and understanding of their function is limited[115, 116]. They can function as ligand sinks and dominant negative forms, but they can also function independently of full-length Trks to influence calcium levels, growth cone extension and dendritic growth and are linked to psychiatric disorders, e.g. depression[117-124]. Like Keks, perhaps kinase-less Trks could regulate brain plasticity vs. degeneration. A functional relationship between NTs and TLRs could exist also in humans, as in cell culture, human BDNF and NGF can induce signalling from a TLR[46] and NGF also functions in immunity and neuroinflammation[125, 126]. Importantly, TLRs can regulate cell survival, death and proliferation, neurogenesis, neurite growth and collapse, learning and memory[23]. They are linked to neuroinflammation, psychiatric disorders, neurodegenerative diseases and stroke[23, 127, 128]. Intriguingly, genome-wide association studies (GWAS) have revealed the involvement of TLRs in various brain conditions and potential links between NTs and TLRs in, for example, major depression[129-132]. Importantly, alterations in NT function underlie psychiatric, neurologic and neurodegenerative brain diseases[13, 15-17, 27, 85, 97, 133, 134] and BDNF underlies the plasticity inducing function of anti-depressants[17, 27, 85]. It is compelling to find out whether and how these important protein families – NTs, TLRs and kinase-less Trks - interact in the human brain.

Conclusion

To conclude, we provide a direct link between structural circuit plasticity and behavioural performance, by a novel molecular mechanism. The neurotrophin DNT-2 and its receptors Toll-6 and the kinase-less Trk family Kek-6 are linked to a dopaminergic circuit. Neuronal activity boosts DNT-2, and DNT-2 and dopamine regulate each other homeostatically. Dopamine labels the circuits engaged and DNT-2, a growth factor, with its receptors Toll-6 and Kek-6, drives structural plasticity in these circuits, enhancing dopamine-dependent behavioural performance. These findings mean that DNT-2 is a plasticity factor in the *Drosophila* brain enabling experience-dependent behavioural enhancement. Whether NTs can similarly functions with TLRs and Kinase-less Trks remains to be explored. As behaviour is a source of experience, this has profound implications for understanding brain function and health.

ACKNOWLEDGEMENTS

We thank our lab, Carolina Rezaval and Thomas Riemensperger for comments on the manuscript; Carolina Rezaval, Reinhard Wolf, Martin Heisenberg and Scott Waddell for advice on - Karina Piotrowska for help with - behaviour experiments; Xiufeng Li for help with programming; Serge Birman, Ann-Shyn Chiang, Ron Davis, André Fialá, Barret Pfeiffer, Xi Rao, Carolina Rezaval, Iris Salecker for flies; DSHB (Iowa) for antibodies; AddGene for plasmids; Bloomington Stock Centre for *Drosophila* stocks. This work was funded by Marie-Curie Sklodowska Post-Doctoral fellowship to J.S.; Science Without Borders-CAPES PhD Studentship BEX 13380/13-3 to SUB; BBSRC Project Grants BB/R00871X/1 and BB/P004997/1 to A.H.; and Wellcome Trust Investigator Award 223197/Z/21/Z to A.H.

AUTHOR CONTRIBUTIONS

J.S., V.C designed and A.H. executed experiments and/or analysed data; S.U-B, G.L, D.S, X.W., F.R.C, M.M. executed experiments and analysed data; M.G.F, S.C., A.H. developed tools; D.K., G.J, V.C., A.H. supervised; J.S and A.H. wrote the manuscript. A.H. conceived and directed the project. All authors provided feedback on, and contributed to improvements to, the manuscript.

DATA AVAILABILITY STATEMENT

All data are contained within the manuscript; metadata and statistical analysis details including full genotypes, sample sizes, statistical tests and p values have been provided in Table S2. This work generated fly stocks and molecular constructs, which we will distribute on request. Raw data will be distributed on request.

DECLARATION OF INTERESTS

The authors declare that they have no conflict of interest.

MATERIALS AND METHODS

Genetics

Mutants: *DNT2*^{37} and *DNT2*^{18} are protein null[46, 49]. *Toll6*^{31} is a null mutant allele[47]. **Driver lines:** *DNT2-Gal4* is a CRISPR/Cas9-knock-in allele, with GAL4 at the start of the gene (this work, see below). *Toll-6-Gal4* was generated by RMCE from *MIMIC Toll-6*^{MIO2127}*; kek6-Gal4* from *MIMIC Kek6*^{MI12953}[44, 49]. *MB320C-Gal4 (BSC68253), MB301B-Gal4 (BSC68311), R58E02-Gal4 (BSC41347), MB247-Gal80 (BSC64306), R58E02-LexA (BSC52740), R14C08-LexA (BSC52473)* were from the *Drosophila* Bloomington Stock Centre (BSC). *Dop1R2-LexA, Dop2R-LexA, Gad-LexA* were kindly provided by Yi Rao; *TH-LexA* (gift of Ron Davis), *TH-Gal4,R58E02-GAL4* (gift of Serge Birman); *G0431-Gal4 (DAL-GAL4), VT49239 nls LexA (DAL LexA)* (gifts from Ann-Shyn Chiang); tubGal80ts, Tdc-LexA. **Reporter lines:** *UAS-CD8::GFP,* for membrane tethered GFP; *UAS-histone-YFP*, for YFP-tagged nuclear histone; *UASFlybow1.1*, constant membrane tethered expression (gift of Iris Salecker); *13xLexAop-nls-tdTomato,* nuclear Tomato (gift of B. Pfeiffer); *UASCD8::RFP, LexAopCD8::GFP* (BSC32229), for dual binary expression; *UAS-homer-GCaMP* for post-synaptic densities (gift of André Fialá), *UAS-syt.eGFP* (BSC6925) and *LexAop-Syt-GCaMP* (BSC64413) for presynaptic sites. **For connectivity*:*** *UAS-DenMarkRFP, UAS-Dsyd1GFP* (gift of Carolina Rezaval); TransTango: *yw UAS-myrGFP,QUAS-mtdTomato-3xHA attP8; Trans-Tango@attP40* (BSC77124); BAcTrace 806 *(w;LexAop2-Syb::GFP-P10(VK37) LexAop-QF2::SNAP25::HIVNES::Syntaxin(VK18)/CyO; UAS-B3Recombinase (attP2) UAS<B3Stop<BoNT/A (VK5)*

UAS<B3Stop<BoNT/A(VK27) QUAS-mtdTomato::HA/TM2): **MCFO clones**: *hs-FLPG5.PEST;; 10xUAS (FRT.stop) myr::smGdP-OLLAS 10xUAS (FRT.stop) myr::smGdP-HA 10xUAS (FRT.stop) myr::smGdP-V5-THS-10xUAS (FRT.stop) myr::smGdP-FLAG* (BSC64086). **Optogenetic activation:** *20x UAS-V5-Syn-CsChrimson td tomato* (gift of B. Pfeiffer**). For thermogenetic activation:** *UASTrpA1@attP2 (BSC26264)* and *UAS-TrpA1@attP216 (BSC26263).* **UAS gene over-expression**: *UAS-DNT2CK, UAS-DNT2FL-GFP, UAS-DNT2-FL-47C, UAS-Toll-6^{CY}*[46, 47]. **UAS-RNAi knockdown:** *UAS-DNT2RNAi* (VDRC49195), *UAS-Toll6RNAi* (VDRC928), *y^{1}v^1; UAS-Toll6RNAi[Trip.HMS04251]* (BSC 56048*), UAS-kek6RNAi* (VDCR 109681), *y^{1}v^1; UAS-Dop2R-RNAi[TRiP.HMC02988](*BSC50621).

Molecular biology

DNT-2GAL4 was generated by CRISPR/Cas9 enhanced homologous recombination. 1 kb long 5' and 3' homology arms (HA) were amplified by PCR from genomic DNA of wild type flies, using primers for 5'HA: atcgcaccggtttttacaggcaccccatgtctga containing AgeI cutting site and cttgacgcggccgcTGTCAATTCATTCGCCGTCGAT containing NotI cutting site. 3'HA primers were: tattaggcgcgccATGACAAAAAGTATTAAACGTCCGCCC containing AscI cutting site and tactcgactagtgaagcacacccaaaatacccagg containing SpeI cutting site. HAs were sequentially cloned by conventional cloning into pGEM-T2AGal4 vector (Addgene #62894). For gRNA cloning, two 20 nucleotide gRNA oligos (gtcGACAAGTTCTTCTTACCTATG and aaacCATAGGTAAGAAGAACTTGTC) were designed using Optimal Target Finder. BbsI enzyme sites were added: gtc(g) at the 5' end of sense oligo, and aaac at the 5' end of the antisense oligo. gRNA is located at 41 bp downstream of the start codon of DNT-2 within the first coding exon. The gRNA was cloned into pU6.3 using conventional ligation. The two constructs were injected in Cas9 bearing flies and red fluorescent (3xP3-RFP) transformants were selected and balanced, after which 3xP3-RFP was removed with CRE-recombinase.

qRT-PCR

qRT-PCR was carried out from 20 whole adult fruit-fly heads, frozen in liquid nitrogen before homogenising in 50 ml Trizol (Ambion #AM9738), followed by a stand RNA extraction protocol. RNA was treated with DNase treatment (ThermoFisher # AM1906) to remove genomic DNA. 200 ng of RNA was used for cDNA synthesis following Goscript Reverse Transcriptase (Promega #237815) protocol. Sample was diluted 1:4 with Nuclease free H_2O. Standard qPCR was performed with SensiFast syb Green Mix (Bioline #B2092020) in ABI qPCR plate (GeneFlow #P3-0292) and machine. To amplify TH mRNA the following primers were used: TH-F: CGAGGACGAGATTTTGTTGGC and TH-R: TTGAGGCGGACCACCAAAG. GAPDH was used as a housekeeping control. Reactions were performed in triplicate. Specificity and size of amplification products were assessed by melting curve analyses. Target gene expression relative to reference gene is expressed as value of $2^{-\Delta\Delta Ct}$ (where Ct is the crossing threshold).

Conditional expression

Multiple Colour Flip Out clones: *DNT2-Gal4, Toll6-Gal4* and *kek6-Gal4* were crossed with *hsFLP::PEST;;MCFO* flies, female offspring were collected and heat-shocked at 37°C in a water bath for 15 mins, then kept for 48h at 25°C before dissecting their brains. ***TransTango:*** DNT2-Gal4 or Oregon female virgins were crossed with *TransTango* males, progeny flies were raised at 18°C constantly and 15 days after eclosion, female flies were selected for immunostaining. **Thermogenetic activation with *TrpA1:*** Fruit-flies were bred at 18°C from egg laying to 4 days post-adult eclosion, then shifted to 29°C in a water bath for 24h followed by 24h recovery at room temperature for over-expressed *DNT-2FL-GFP*; for the other experiments, after breeding as above, adult flies were transferred to an incubator at 30°C, kept there for 24h and then brains were dissected. **Conditional gene over-expression and RNAi knockdown:** Flies bearing the temperature sensitive GAL4 repressor tubGal80^{ts} were kept at 18°C from egg laying to adult eclosion, then transferred to 30 °C incubator for 48h for Dcp-1+ and cell counting experiments and for 120h for TH+ cell counting.

Immunostainings

Adult fruit-fly female brains were dissected (in PBS), fixed (in 4% para-formaldehyde, room temperature, 20-30min) and stained following standard protocols. Primary antibodies and their dilutions were as follows: Mouse anti-Brp (nc82) 1:10 (DSHB); Rabbit anti-GFP 1:250 (Thermofisher); Mouse anti-GFP 1:250 (Thermofisher); Chicken anti-GFP 1:500 (Aves); Rabbit anti-FLAG 1:50 (Sigma); Mouse anti-V5 1:50 (Invitrogen); Chicken anti-HA 1:50 (Aves); Rabbit anti-VGlut 1:500 (gift of Hermann); Mouse anti-TH 1:250 (Immunostar); Rabbit anti-TH 1:250 (Novus Biologicals); Rabbit anti-DsRed 1:250 (Clontek); Mouse anti-ChAT4B1 1:250 (DSHB); Rabbit anti-5-HT 1:500 (Immunostar); Rabbit Anti-DCP-1 1:250 (Cell Signalling). Seconday antibodies were all used at 1:500 and all were from Thermofisher: Alexa Flour 488 Goat anti-mouse, Alexa Flour 488 donkey anti-rabbit, Alexa Flour 488 Goat anti-rabbit (Fab')2, Alexa Flour 488 Goat anti-chicken, Alexa Four 546 Goat anti-rabbit, Alexa Four 546 Goat anti-mouse, Alex Four 647 Goat anti-rabbit, Alex Four 647 Goat anti-mouse.

Microscopy and Imaging

Laser scanning confocal microscopy. Stacks of microscopy images were acquired using laser scanning confocal microscopy with either Zeiss LSM710, 900 or Leica SP8. Brains were scanned with a resolution of 1024x1024, with Leica SP8 20x oil objective and 1 mm step for whole brain and DCP-1 stainings, 40x oil objective and 1 mm step for central brain. Resolution of 1024x512 was used for analysing PAM clusters with 0.96 mm step for cell counting; 0.5 mm step for neuronal morphology; and 63x oil objective with 0.5mm step for neuronal connections. Acquisition speed in Leica SP8 was 400Hz, with no line averaging. Resolution of 3072x3072 was used for single image analysis of synapses, using either Leica SP8 or Zeiss LSM900 and Airyscan acquisition with 40x water objective speed 6, and average 4, or with 1024x512, with 40x oil lens 2x zoom and 0.35mm step. TH counting in PAM were scanned with Zeiss 710 with a resolution 1024x1024, 40x oil objective, step 1 mm, speed 8. Zeiss LSM900 Airyscan with a resolution of 1024x1024, 40x water objective, speed 7, 0.7 zoom and 0.31µm step size was used for acquisition of optical sections of synapses in PAM neurons.

Optogenetics and Epac1 FRET 2-photon imaging

To test whether DNT-2 neurons can respond to dopamine via the Dop2R inhibitory receptor, we used the cAMP sensor Epac1 and 2-photon confocal microscopy. Epac1 is FRET probe, whereby data are acquired from CFP and YFP emission and lower YFP/CFP ratio reveals higher cAMP levels. DNT-2Gal4 flies were crossed to *UAS-CsChrimson UAS Epac1* flies, to stimulate DNT-2 neurons and detect cAMP levels in DNT2 neurons. 1-3 day-old *DNT2Gal4>UASCsChrimson, UAS Epac1* flies were collected and separated in two groups. Flies bearing *DNT2Gal4 UASCsChrimson UAS Epac1 UASDop2RRNAi* were fed on 50μM all-trans retinal food for at least 3 days prior to imaging and kept in constant darkness prior to the experiment.

Optogenetic stimulation of fly brains expressing CsChrimson in DNT-2 neurons was carried out using a sapphire 588nm laser, in a 2-photon confocal microscope. For acquisition of YFP and CFP data from Epac1 samples, a FV30-FYC filter was applied, using a 925nm laser for both YFP and CFP imaging. The stimulation laser was targeted onto DNT-2 neuron projections in SMP region for 20s. Acquisition ROI was at DNT-2A cell bodies with a frame rate of around 10Hz. The first acquisition started 10s before the 20s stimulation and consequential acquisition was done every 30s for 10 cycles.

Image analysis of Epac data was carried out using ImageJ. The two channels (YFP and CFP) were separated, and the ratio of YFP/CFP for each pixel was calculated using the ImageJ>Image Calculator by diving YFP channel by CFP channel. The obtained result of YFP/CFP ratio was saved and the mean ratio of YFP/CFP in the ROI was calculated for each time point and 11 time points were used. The 11 values represent the ratio of YFP/CFP change in the cell body upon stimulation, with 30s interval and repeated 10 times.

Automatic cell counting with DeadEasy plug-ins: To automatically count cell number labelled with nuclear reporters (e.g. Histone-YFP, nls-tdTomato) and Dcp-1+ cells, we adapted the DeadEasy Central Brain ImageJ plug-in[44]. DeadEasy automatically identifies and counts cells labelled with nuclear reporters in 3D stacks of confocal image in the adult central brain. Brains expressing these reporters were dissected, fixed and scanned without stainings. DeadEasy Central Brain was used with threshold set to 75.

To count the TH labelled PAMs, we purposely developed a newly plug-in called DeadEasy DAN. Since TH-stained images had Poisson noise, a median filter was used to reduce noise, without having large

losses at the edges. Then, given that cell walls of irregular intensity are frequently encountered, a 3D morphological closing was performed. Since each cell is identified as a dark area surrounded by pixels of higher intensity and that, in the background, due to noise, it is also possible to find local minima that can be incorrectly identified as cells, all very dark pixels were assigned a value of zero. To mark each cell, each chasm in the image was found using a 3D extended h-minimal transform. As more than one local minimum can be found within each cell, which would result in counting a cell multiple times, a 3D inverse dome detection was performed, and then labelled. Thus, each inverse dome was used as a seed to identify each cell. Once the seeds were obtained, a 3D watershed transformation was performed to recover the shape of the cells. Finally, a colour palette was used to visualize each cell more easily. DeadEasy DAN is accurate in controls and mutants, but less accurate with RNAi knock-down genotypes, for which it was not used and TH+ cells were counted manually instead, assisted by the ImageJ cell counter.

Dendrite analysis with Imaris: To analyze dendritic complexity, image data were processed with Imaris using the "Filament Autodetect" function with the default algorithm and autopatch function. Setting of the threshold was consistent within the same experiment: the largest or smallest diameter of the dendrite, same threshold for background substation, local contrast. Number of dendritic branches, dendritic segments, dendritic branch points and dendritic terminal points were collected to compare the difference between the groups.

Vesicles, synapses and PSD analysis with Imaris: To analyse the number and volume of Homer-GCaMP GFP+ post-synaptic densities (PSD), Syt-GCaMP GFP+ presynaptic sites and DNT-2FLGFP+ vesicles, optical section images of confocal stacks through the brain were processed with the Imaris Spot function. Setting of the threshold was consistent across genotypes.

Behaviour

1. Startle induced negative geotaxis Assay was carried out as described in [88]. Groups of approximately 10 male flies of the same genotype were placed in a fresh tube one night before the test, after which flies were transferred to a column formed with two empty tubes 15cm long and 2cm and then habituated for

30mins. Columns were tapped 3-4 times, flies fell to the bottom and then climbed upwards. Multiple rounds of testing were performed 3-7 times in a row per column. The process was filmed and films were analysed. Flies were scored during the first 15s after the tapping, and those that climbed above 13cm and those that climbed below 2cm were counted separately. Results given are mean ± SEM of the scores obtained with ten groups of flies per genotype. The performance index (PI) is defined as $1/2[(n_{tot} + n_{top} - n_{bot})/n_{tot}]$, where n_{tot}, n_{top}, and n_{bot} are the total number of flies, the number of flies at the top, and the number of flies at the bottom, respectively. The assay was carried out at 25°C, 55% humidity. Flies with tubGal80^{ts} to conditionally overexpress or knock-down were shifted from 18 to 30°at eclosion and kept for 5 days at 30°C to induce Gal4. Experiments were carried in an environmental chamber at 31°C, 60% humidity or in a humidity and temperature-controlled behaviour lab always kept at 25°C.

2. Spontaneous Locomotion in an open arena: Male flies of each genotype were collected and kept in groups of 10-20 flies, in vials containing fresh fly food for 5-9 days. Before filming, three male flies from one genotype were transferred into a 24 mm well of a multi-well plate using an aspirator and habituated for 15 – 20 mins. The multi-well plate with transparent lid and bottom was placed on a white LED light pad (XIAOSTAR Light Box) and either inside a light-shielding black box (PULUZ, 40*40*40cm) in a room with constant temperature (25°C) and humidity (55%) to maintain stable environmental conditions (Figure 7D), or inside a temperature controlled environmental chamber at 18°C or 30°C (Figure 7E,F,) . The locomotion behaviour of freely-moving flies was filmed with a camera (Panasonic, HC-V260) in the morning from ZT1-ZT4 and for 10 min at a frame-rate of 25 fps. The 10-min videos were trimmed (from 00:02:00 to 00:07:00) to 5-min videos for analysis using Flytracker software[89]. For the *DNT-2* mutants and over-expression of Toll-6^{CY} experiments, flies were bred and tested at 25 °C. To test over-expression of *DNT-2* with *tubGAL80^{ts}; DNT2-Gal4>UAS-DNT-2FL*, flies were raised at 18°C until eclosion, and controls were kept and tested at 18°C; test groups were transferred directly after eclosion to 30°C for 5 days and were tested in an environmental chamber kept at 30°C, 60%. For thermo-genetic activation of DNT2 neurons using TrpA1 (DNT-2GAL4>UASTrpA1), flies were bred at 18°C and kept at 18°C for 7-9 days post-eclosion. Following habituation at 18°c for 20 mins in the multi-well plates, they were transferred to the 30°C chamber 10 mins before filming to activate TrpA1 and then filmed for the following

10 minutes. Fly locomotion activity was tracked using FlyTracker and calculated (distance and speed) in Matlab[89] using the raw data generated from the tracking procedure. The "walking distance" was calculated as the sum of the distance flies moved and the "walking speed" was the speed of flies only when they were walking, and it was calculated using only frames where flies moved above 4 mm/s (which corresponds to two body lengths).

3. Appetitive long term memory test: Appetitive long-term memory was tested as described in Krashes and Waddell[91]. The two conditioning odours used were isoamyl acetate, Sigma-Aldrich #24900822, 6mL in 8mL mineral oil (Sigma-Aldrich #330760) and 4-methylcyclohexanol (Sigma-Aldrich # 153095, 10mL in 8mL mineral oil). Groups of 80-120 mixed sex flies were starved in a 1% agar tube filled with a damp 20 x 60 mm piece of filter paper for 18-20 hour before conditioning. During conditioning training, one odorant was presented with a dry filter paper (unconditioned odour, CS-) for 2 minutes, before a 30 second break, and presentation of a second odorant with filter paper coated with dry sucrose (conditioned odour, CS+). The test was repeated pairing the other odorant with sucrose, with a different group of flies to form one replicate. After training, flies were transferred back to agar tubes for testing 24 hours later. Performance index (PI) was calculated in the same way as in Krashes and Waddell[91], as the number of flies approaching the conditioned odour minus the number of flies going in the opposite direction, divided by the total number of flies. A single PI values is the average score from the test with the reverse conditioning odour combination. Groups for which the total number of flies among both odorants was below 15 were discarded. For the *DNT-2* over-expression experiments with *tubGAL80^{ts}; DNT-2>DNT-2FL,* flies were raised at 18°C until 7-9 days post-eclosion. They were then either transferred to and maintained at 23°C (controls) or 30°C for 18-20h starvation, training, and up to testing 24h later.

Statistical analysis: Statistical analyses were carried out using Graph-Pad Prism. Confidence interval was 95%, setting significance at $p<0.05$. Chi-square tests were carried out when comparing categorical data. Numerical data were tested first for their type of distributions. If data were distributed normally, unpaired Student t-tests were used to compare means between two groups and One Way ANOVA or Welch ANOVA for larger groups, followed by post-doc Dunnett test for multiple comparisons to a fixed control. Two Way

ANOVA was used when comparisons to two variables were made. If data were not normally distributed, non-parametric Mann-Whitney U-test for 2 two group comparisons and Kruskal Wallis ANOVA for larger groups, followed by post-hoc Dunn's multiple comparisons test to a fixed control. Statistical details including full genotypes, sample sizes, tests and p values are provided in Supplementary Table S2.

REFERENCES

1. Feldman, D.E. and M. Brecht, *Map plasticity in somatosensory cortex.* Science, 2005. **310**(5749): p. 810-5.

2. Gage, F.H., *Adult neurogenesis in mammals.* Science, 2019. **364**(6443): p. 827-828.

3. Holtmaat, A. and K. Svoboda, *Experience-dependent structural synaptic plasticity in the mammalian brain.* Nat Rev Neurosci, 2009. **10**(9): p. 647-58.

4. Wiesel, T.N., *Postnatal development of the visual cortex and the influence of environment.* Nature, 1982. **299**(5884): p. 583-91.

5. Bharmauria, V., et al., *Adaptation-induced plasticity in the sensory cortex.* J Neurophysiol, 2022. **128**(4): p. 946-962.

6. Chen, C.C. and J.C. Brumberg, *Sensory Experience as a Regulator of Structural Plasticity in the Developing Whisker-to-Barrel System.* Frontiers in Cellular Neuroscience, 2021. **15**.

7. Cotman, C.W. and N.C. Berchtold, *Exercise: a behavioral intervention to enhance brain health and plasticity.* Trends Neurosci, 2002. **25**(6): p. 295-301.

8. Maguire, E.A., et al., *Navigation-related structural change in the hippocampi of taxi drivers.* Proc Natl Acad Sci U S A, 2000. **97**(8): p. 4398-403.

9. Sur, M. and J.L. Rubenstein, *Patterning and plasticity of the cerebral cortex.* Science, 2005. **310**(5749): p. 805-10.

10. Woollett, K. and E.A. Maguire, *Acquiring "the Knowledge" of London's layout drives structural brain changes.* Curr Biol, 2011. **21**(24): p. 2109-14.

11. Kuner, R. and H. Flor, *Structural plasticity and reorganisation in chronic pain.* Nat Rev Neurosci, 2016. **18**(1): p. 20-30.

12. Leemhuis, E., L. De Gennaro, and A.M. Pazzaglia, *Disconnected Body Representation: Neuroplasticity Following Spinal Cord Injury.* J Clin Med, 2019. **8**(12).

13. Yang, T., et al., *The Role of BDNF on Neural Plasticity in Depression.* Front Cell Neurosci, 2020. **14**: p. 82.

14. Poo, M.M., *Neurotrophins as synaptic modulators.* Nat Rev Neurosci, 2001. **2**(1): p. 24-32.

15. Lu, B., P.T. Pang, and N.H. Woo, *The yin and yang of neurotrophin action.* Nat Rev Neurosci, 2005. **6**(8): p. 603-14.

16. Park, H. and M.M. Poo, *Neurotrophin regulation of neural circuit development and function.* Nat Rev Neurosci, 2013. **14**(1): p. 7-23.

17. Casarotto, P.C., et al., *Antidepressant drugs act by directly binding to TRKB neurotrophin receptors.* Cell, 2021. **184**(5): p. 1299-1313 e19.

18. Castren, E. and L. Monteggia, *Brain-Derived Neurotrophic Factor Signaling in Depression and Antidepressant Action.* Biol Psychiatry, 2021.

19. Squillace, S. and D. Salvemini, *Toll-like receptor-mediated neuroinflammation: relevance for cognitive dysfunctions.* Trends Pharmacol Sci, 2022. **43**(9): p. 726-739.

20. Gay, N.J. and M. Gangloff, *Structure and function of Toll receptors and their ligands.* Annu Rev Biochem, 2007. **76**: p. 141-65.

21. Ma, Y., et al., *Toll-like receptor 8 functions as a negative regulator of neurite outgrowth and inducer of neuronal apoptosis.* J Cell Biol, 2006. **175**(2): p. 209-15.

22. Okun, E., et al., *Toll-like receptor 3 inhibits memory retention and constrains adult hippocampal neurogenesis.* Proc Natl Acad Sci U S A, 2010. **107**(35): p. 15625-30.

23. Okun, E., K.J. Griffioen, and M.P. Mattson, *Toll-like receptor signaling in neural plasticity and disease.* Trends Neurosci, 2011. **34**(5): p. 269-81.

24. Rolls, A., et al., *Toll-like receptors modulate adult hippocampal neurogenesis.* Nat Cell Biol, 2007. **9**(9): p. 1081-8.

25. Patel, V., A.M. Patel, and J.J. McArdle, *Synaptic abnormalities of mice lacking toll-like receptor (TLR)-9.* Neuroscience, 2016. **324**: p. 1-10.

26. Chen, C.Y., et al., *Beyond defense: regulation of neuronal morphogenesis and brain functions via Toll-like receptors.* J Biomed Sci, 2019. **26**(1): p. 90.

27. Wang, C.S., E.T. Kavalali, and L.M. Monteggia, *BDNF signaling in context: From synaptic regulation to psychiatric disorders.* Cell, 2022. **185**(1): p. 62-76.

28. Baltruschat, L., et al., *Circuit reorganization in the Drosophila mushroom body calyx accompanies memory consolidation.* Cell Rep, 2021. **34**(11): p. 108871.

29. Barth, M. and M. Heisenberg, *Vision affects mushroom bodies and central complex in Drosophila melanogaster.* Learn Mem, 1997. **4**(2): p. 219-29.

30. Barth, M., et al., *Experience-dependent developmental plasticity in the optic lobe of Drosophila melanogaster.* J Neurosci, 1997. **17**(4): p. 1493-504.

31. Coban, B., et al., *The caloric value of food intake structurally adjusts a neuronal mushroom body circuit mediating olfactory learning in Drosophila.* Learn Mem, 2024. **31**(5).

32. Kremer, M.C., et al., *Structural long-term changes at mushroom body input synapses.* Curr Biol, 2010. **20**(21): p. 1938-44.

33. Linneweber, G.A., et al., *A neurodevelopmental origin of behavioral individuality in the Drosophila visual system.* Science, 2020. **367**(6482): p. 1112-1119.

34. Sachse, S., et al., *Activity-dependent plasticity in an olfactory circuit.* Neuron, 2007. **56**(5): p. 838-50.

35. Sugie, A., et al., *Molecular Remodeling of the Presynaptic Active Zone of Drosophila Photoreceptors via Activity-Dependent Feedback.* Neuron, 2015. **86**(3): p. 711-25.

36. Technau, G.M., *Fiber number in the mushroom bodies of adult Drosophila melanogaster depends on age, sex and experience.* J Neurogenet, 1984. **1**(2): p. 113-26.

37. Devaud, J.M., A. Acebes, and A. Ferrus, *Odor exposure causes central adaptation and morphological changes in selected olfactory glomeruli in Drosophila.* J Neurosci, 2001. **21**(16): p. 6274-82.

38. Gorska-Andrzejak, J., et al., *Structural daily rhythms in GFP-labelled neurons in the visual system of Drosophila melanogaster.* Photochem Photobiol Sci, 2005. **4**(9): p. 721-6.

39. Bushey, D., G. Tononi, and C. Cirelli, *Sleep and synaptic homeostasis: structural evidence in Drosophila.* Science, 2011. **332**(6037): p. 1576-81.

40. Vaughen, J.P., et al., *Glial control of sphingolipid levels sculpts diurnal remodeling in a circadian circuit.* Neuron, 2022. **110**(19): p. 3186-3205 e7.

41. Fernandez, M.P., J. Berni, and M.F. Ceriani, *Circadian remodeling of neuronal circuits involved in rhythmic behavior.* PLoS Biol, 2008. **6**(3): p. e69.

42. Duhart, J.M., et al., *Circadian Structural Plasticity Drives Remodeling of E Cell Output.* Curr Biol, 2020. **30**(24): p. 5040-5048 e5.

43. Bolus, H., et al., *Modeling Neurodegenerative Disorders in Drosophila melanogaster.* Int J Mol Sci, 2020. **21**(9).

44. Li, G., et al., *A Toll-receptor map underlies structural brain plasticity.* Elife, 2020. **9**.

45. Anthoney, N., I. Foldi, and A. Hidalgo, *Toll and Toll-like receptor signalling in development.* Development, 2018. **145**(9).

46. Foldi, I., et al., *Three-tier regulation of cell number plasticity by neurotrophins and Tolls in Drosophila.* J Cell Biol, 2017. **216**(5): p. 1421-1438.

47. McIlroy, G., et al., *Toll-6 and Toll-7 function as neurotrophin receptors in the Drosophila melanogaster CNS.* Nat Neurosci, 2013. **16**(9): p. 1248-56.

48. McLaughlin, C.N., et al., *A Toll receptor-FoxO pathway represses Pavarotti/MKLP1 to promote microtubule dynamics in motoneurons.* J Cell Biol, 2016. **214**(4): p. 459-74.

49. Ulian-Benitez, S., et al., *Kek-6: A truncated-Trk-like receptor for Drosophila neurotrophin 2 regulates structural synaptic plasticity.* PLoS Genet, 2017. **13**(8): p. e1006968.

50. Ward, A., et al., *Toll receptors instruct axon and dendrite targeting and participate in synaptic partner matching in a Drosophila olfactory circuit.* Neuron, 2015. **85**(5): p. 1013-28.

51. Meyer, S.N., et al., *An ancient defense system eliminates unfit cells from developing tissues during cell competition.* Science, 2014. **346**(6214): p. 1258236.

52. Pare, A.C., et al., *A positional Toll receptor code directs convergent extension in Drosophila.* Nature, 2014. **515**(7528): p. 523-7.

53. Tamada, M., et al., *Toll receptors remodel epithelia by directing planar-polarized Src and PI3K activity.* Dev Cell, 2021. **56**(11): p. 1589-1602 e9.

54. Riemensperger, T., et al., *Behavioral consequences of dopamine deficiency in the Drosophila central nervous system.* Proc Natl Acad Sci U S A, 2011. **108**(2): p. 834-9.

55. Waddell, S., *Reinforcement signalling in Drosophila; dopamine does it all after all.* Curr Opin Neurobiol, 2013. **23**(3): p. 324-9.

56. Adel, M. and L.C. Griffith, *The Role of Dopamine in Associative Learning in Drosophila: An Updated Unified Model.* Neurosci Bull, 2021. **37**(6): p. 831-852.

57. Aso, Y., et al., *The neuronal architecture of the mushroom body provides a logic for associative learning.* Elife, 2014. **3**: p. e04577.

58. Boto, T., A. Stahl, and S.M. Tomchik, *Cellular and circuit mechanisms of olfactory associative learning in Drosophila.* J Neurogenet, 2020. **34**(1): p. 36-46.

59. Chen, C.C., et al., *Visualizing long-term memory formation in two neurons of the Drosophila brain.* Science, 2012. **335**(6069): p. 678-85.

60. Aso, Y., et al., *Mushroom body output neurons encode valence and guide memory-based action selection in Drosophila.* Elife, 2014. **3**: p. e04580.

61. Heisenberg, M., *Mushroom body memoir: from maps to models.* Nat Rev Neurosci, 2003. **4**(4): p. 266-75.

62. Guven-Ozkan, T. and R.L. Davis, *Functional neuroanatomy of Drosophila olfactory memory formation.* Learn Mem, 2014. **21**(10): p. 519-26.

63. Weber, A.N., et al., *Binding of the Drosophila cytokine Spatzle to Toll is direct and establishes signaling.* Nat Immunol, 2003. **4**(8): p. 794-800.

64. Hoffmann, A., et al., *Biophysical characterization of refolded Drosophila Spatzle, a cystine knot protein, reveals distinct properties of three isoforms.* J Biol Chem, 2008. **283**(47): p. 32598-609.

65. Hoffmann, A., et al., *Crystallization of Spatzle, a cystine-knot protein involved in embryonic development and innate immunity in Drosophila melanogaster.* Acta Crystallogr Sect F Struct Biol Cryst Commun, 2008. **64**(Pt 8): p. 707-10.

66. Lewis, M., et al., *Cytokine Spatzle binds to the Drosophila immunoreceptor Toll with a neurotrophin-like specificity and couples receptor activation.* Proc Natl Acad Sci U S A, 2013. **110**(51): p. 20461-6.

67. DeLotto, Y. and R. DeLotto, *Proteolytic processing of the Drosophila Spatzle protein by easter generates a dimeric NGF-like molecule with ventralising activity.* Mech Dev, 1998. **72**(1-2): p. 141-8.

68. Zhu, B., et al., *Drosophila neurotrophins reveal a common mechanism for nervous system formation.* PLoS Biol, 2008. **6**(11): p. e284.

69. Sutcliffe, B., et al., *Neuron-type specific functions of DNT1, DNT2 and Spz at the Drosophila neuromuscular junction.* PLoS One, 2013. **8**(10): p. e75902.

70. Costa, M., et al., *NBLAST: Rapid, Sensitive Comparison of Neuronal Structure and Construction of Neuron Family Databases.* Neuron, 2016. **91**(2): p. 293-311.

71. Nern, A., B.D. Pfeiffer, and G.M. Rubin, *Optimized tools for multicolor stochastic labeling reveal diverse stereotyped cell arrangements in the fly visual system.* Proc Natl Acad Sci U S A, 2015. **112**(22): p. E2967-76.

72. Mayseless, O., et al., *Developmental Coordination during Olfactory Circuit Remodeling in Drosophila.* Neuron, 2018. **99**(6): p. 1204-1215 e5.

73. Heisenberg, M., M. Heusipp, and C. Wanke, *Structural plasticity in the Drosophila brain.* J Neurosci, 1995. **15**(3 Pt 1): p. 1951-60.

74. Croset, V., C.D. Treiber, and S. Waddell, *Cellular diversity in the Drosophila midbrain revealed by single-cell transcriptomics.* Elife, 2018. **7**.

75. Boto, T., et al., *Dopaminergic modulation of cAMP drives nonlinear plasticity across the Drosophila mushroom body lobes.* Curr Biol, 2014. **24**(8): p. 822-31.

76. Talay, M., et al., *Transsynaptic Mapping of Second-Order Taste Neurons in Flies by trans-Tango.* Neuron, 2017. **96**(4): p. 783-795 e4.

77. Cachero, S., et al., *BAcTrace a new tool for retrograde tracing of neuronal circuit.* Nature Methods, 2020. **17**: p. 1254-1261.

78. Neve, K.A., J.K. Seamans, and H. Trantham-Davidson, *Dopamine receptor signaling.* J Recept Signal Transduct Res, 2004. **24**(3): p. 165-205.

79. Hearn, M.G., et al., *A Drosophila dopamine 2-like receptor: Molecular characterization and identification of multiple alternatively spliced variants.* Proc Natl Acad Sci U S A, 2002. **99**(22): p. 14554-9.

80. Shafer, O.T., et al., *Widespread receptivity to neuropeptide PDF throughout the neuronal circadian clock network of Drosophila revealed by real-time cyclic AMP imaging.* Neuron, 2008. **58**(2): p. 223-37.

81. Liu, C., et al., *A subset of dopamine neurons signals reward for odour memory in Drosophila.* Nature, 2012. **488**(7412): p. 512-6.

82. Feany, M.B. and W.W. Bender, *A Drosophila model of Parkinson's disease.* Nature, 2000. **404**(6776): p. 394-8.

83. Aso, Y., et al., *Three dopamine pathways induce aversive odor memories with different stability.* PLoS Genet, 2012. **8**(7): p. e1002768.

84. Placais, P.Y., et al., *Slow oscillations in two pairs of dopaminergic neurons gate long-term memory formation in Drosophila.* Nat Neurosci, 2012. **15**(4): p. 592-9.

85. Lu, B., et al., *BDNF-based synaptic repair as a disease-modifying strategy for neurodegenerative diseases.* Nat Rev Neurosci, 2013. **14**(6): p. 401-16.

86. Fuentes-Medel, Y., et al., *Glia and muscle sculpt neuromuscular arbors by engulfing destabilized synaptic boutons and shed presynaptic debris.* PLoS Biol, 2009. **7**(8): p. e1000184.

87. Riemensperger, T., et al., *A single dopamine pathway underlies progressive locomotor deficits in a Drosophila model of Parkinson disease.* Cell Rep, 2013. **5**(4): p. 952-60.

88. Sun, J., et al., *Neural Control of Startle-Induced Locomotion by the Mushroom Bodies and Associated Neurons in Drosophila.* Front Syst Neurosci, 2018. **12**: p. 6.

89. Eyjolfsdottir, E., et al. *Detecting Social Actions of Fruit Flies*. 2014. Cham: Springer International Publishing.

90. Krashes, M.J. and S. Waddell, *Rapid consolidation to a radish and protein synthesis-dependent long-term memory after single-session appetitive olfactory conditioning in Drosophila.* J Neurosci, 2008. **28**(12): p. 3103-13.

91. Krashes, M.J. and S. Waddell, *Drosophila appetitive olfactory conditioning.* Cold Spring Harb Protoc, 2011. **2011**(5): p. pdb prot5609.

92. Zhang, J., et al., *Maintaining Toll signaling in Drosophila brain is required to sustain autophagy for dopamine neuron survival.* iScience, 2024. **27**(2): p. 108795.

93. McLaughlin, C.N., et al., *Dying Neurons Utilize Innate Immune Signaling to Prime Glia for Phagocytosis during Development.* Dev Cell, 2019. **48**(4): p. 506-522 e6.

94. Li, G. and A. Hidalgo, *The Toll Route to Structural Brain Plasticity.* Front Physiol, 2021. **12**: p. 679766.

95. Pech, U., et al., *Optical dissection of experience-dependent pre- and postsynaptic plasticity in the Drosophila brain.* Cell Rep, 2015. **10**(12): p. 2083-95.

96. Cheng, L.K., et al., *Long-term musical training induces white matter plasticity in emotion and language networks.* Hum Brain Mapp, 2022.

97. Wohleb, E.S., et al., *Integrating neuroimmune systems in the neurobiology of depression.* Nat Rev Neurosci, 2016. **17**(8): p. 497-511.

98. Vahid-Ansari, F. and P.R. Albert, *Rewiring of the Serotonin System in Major Depression.* Front Psychiatry, 2021. **12**: p. 802581.

99. Forrest, M.P., E. Parnell, and P. Penzes, *Dendritic structural plasticity and neuropsychiatric disease.* Nat Rev Neurosci, 2018. **19**(4): p. 215-234.

100. Arnot, C.J., N.J. Gay, and M. Gangloff, *Molecular mechanism that induces activation of Spatzle, the ligand for the Drosophila Toll receptor.* J Biol Chem, 2010. **285**(25): p. 19502-9.

101. Hu, X., et al., *Multimerization and interaction of Toll and Spatzle in Drosophila.* Proc Natl Acad Sci U S A, 2004. **101**(25): p. 9369-74.

102. Arikkath, J., *Molecular mechanisms of dendrite morphogenesis.* Front Cell Neurosci, 2012. **6**: p. 61.

103. Horch, H.W. and L.C. Katz, *BDNF release from single cells elicits local dendritic growth in nearby neurons.* Nat Neurosci, 2002. **5**(11): p. 1177-84.

104. Jenks, K.R., et al., *Heterosynaptic Plasticity and the Experience-Dependent Refinement of Developing Neuronal Circuits.* Front Neural Circuits, 2021. **15**: p. 803401.

105. Minichiello, L., *TrkB signalling pathways in LTP and learning.* Nat Rev Neurosci, 2009. **10**(12): p. 850-60.

106. Lee, J.L., B.J. Everitt, and K.L. Thomas, *Independent cellular processes for hippocampal memory consolidation and reconsolidation.* Science, 2004. **304**(5672): p. 839-43.

107. Blochl, A. and C. Sirrenberg, *Neurotrophins stimulate the release of dopamine from rat mesencephalic neurons via Trk and p75Lntr receptors.* J Biol Chem, 1996. **271**(35): p. 21100-7.

108. Guillin, O., et al., *BDNF controls dopamine D3 receptor expression and triggers behavioural sensitization.* Nature, 2001. **411**(6833): p. 86-9.

109. Sahu, M.P., et al., *Neurotrophin receptor Ntrk2b function in the maintenance of dopamine and serotonin neurons in zebrafish.* Sci Rep, 2019. **9**(1): p. 2036.

110. Hyman, C., et al., *BDNF is a neurotrophic factor for dopaminergic neurons of the substantia nigra.* Nature, 1991. **350**(6315): p. 230-2.

111. Berton, O., et al., *Essential role of BDNF in the mesolimbic dopamine pathway in social defeat stress.* Science, 2006. **311**(5762): p. 864-8.

112. Mandai, K., et al., *LIG family receptor tyrosine kinase-associated proteins modulate growth factor signals during neural development.* Neuron, 2009. **63**(5): p. 614-27.

113. MacLaren, C.M., et al., *Comparative analysis of the Kekkon molecules, related members of the LIG superfamily.* Dev Genes Evol, 2004. **214**(7): p. 360-6.

114. Tauszig, S., et al., *Toll-related receptors and the control of antimicrobial peptide expression in Drosophila.* Proc Natl Acad Sci U S A, 2000. **97**(19): p. 10520-5.

115. Stoilov, P., E. Castren, and S. Stamm, *Analysis of the human TrkB gene genomic organization reveals novel TrkB isoforms, unusual gene length, and splicing mechanism.* Biochem Biophys Res Commun, 2002. **290**(3): p. 1054-65.

116. Fryer, R.H., et al., *Developmental and mature expression of full-length and truncated TrkB receptors in the rat forebrain.* J Comp Neurol, 1996. **374**(1): p. 21-40.

117. Yacoubian, T.A. and D.C. Lo, *Truncated and full-length TrkB receptors regulate distinct modes of dendritic growth.* Nat Neurosci, 2000. **3**(4): p. 342-9.

118. Tessarollo, L. and S. Yanpallewar, *TrkB Truncated Isoform Receptors as Transducers and Determinants of BDNF Functions.* Front Neurosci, 2022. **16**: p. 847572.

119. Fenner, B.M., *Truncated TrkB: beyond a dominant negative receptor.* Cytokine Growth Factor Rev, 2012. **23**(1-2): p. 15-24.

120. Ohira, K. and M. Hayashi, *A new aspect of the TrkB signaling pathway in neural plasticity.* Curr Neuropharmacol, 2009. **7**(4): p. 276-85.

121. Ferrer, I., et al., *BDNF and full-length and truncated TrkB expression in Alzheimer disease. Implications in therapeutic strategies.* J Neuropathol Exp Neurol, 1999. **58**(7): p. 729-39.

122. Carim-Todd, L., et al., *Endogenous truncated TrkB.T1 receptor regulates neuronal complexity and TrkB kinase receptor function in vivo.* J Neurosci, 2009. **29**(3): p. 678-85.

123. Ernst, C., et al., *Alternative splicing, methylation state, and expression profile of tropomyosin-related kinase B in the frontal cortex of suicide completers.* Arch Gen Psychiatry, 2009. **66**(1): p. 22-32.

124. Ohira, K., et al., *TrkB-T1 regulates the RhoA signaling and actin cytoskeleton in glioma cells.* Biochem Biophys Res Commun, 2006. **342**(3): p. 867-74.

125. Hepburn, L., et al., *Innate immunity. A Spaetzle-like role for nerve growth factor beta in vertebrate immunity to Staphylococcus aureus.* Science, 2014. **346**(6209): p. 641-646.

126. Levi-Montalcini, R., et al., *Nerve growth factor: from neurotrophin to neurokine.* Trends Neurosci, 1996. **19**(11): p. 514-20.

127. Adhikarla, S.V., et al., *TLR-Mediated Signal Transduction and Neurodegenerative Disorders.* Brain Sci, 2021. **11**(11).

128. Figueroa-Hall, L.K., M.P. Paulus, and J. Savitz, *Toll-Like Receptor Signaling in Depression.* Psychoneuroendocrinology, 2020. **121**: p. 104843.

129. Sharma, A., *Genome-wide expression analysis in epilepsy: a synthetic review.* Curr Top Med Chem, 2012. **12**(9): p. 1008-32.

130. Chan, R.F., et al., *Cell Type-Specific Methylome-wide Association Studies Implicate Neurotrophin and Innate Immune Signaling in Major Depressive Disorder.* Biol Psychiatry, 2020. **87**(5): p. 431-442.

131. Garrett, M.E., et al., *Gene Expression Analysis in Three Posttraumatic Stress Disorder Cohorts Implicates Inflammation and Innate Immunity Pathways and Uncovers Shared Genetic Risk With Major Depressive Disorder.* Front Neurosci, 2021. **15**: p. 678548.

132. Mehta, D., et al., *Transcriptome analysis reveals novel genes and immune networks dysregulated in veterans with PTSD.* Brain Behav Immun, 2018. **74**: p. 133-142.

133. Krishnan, V. and E.J. Nestler, *The molecular neurobiology of depression.* Nature, 2008. **455**(7215): p. 894-902.

134. Martinowich, K., H. Manji, and B. Lu, *New insights into BDNF function in depression and anxiety.* Nat Neurosci, 2007. **10**(9): p. 1089-93.

FIGURE LEGENDS

Figure 1 Neurons expressing *DNT-2* and its receptors *Toll-6* and *kek-6* in the adult brain

(A) *DNT-2A* expressing neurons (*DNT-2>FlyBow1.1* in green; anti-Brp in magenta) have cell bodies in SOG and project to FLA/PRW and SMP. **(B,D)** Pre-synaptic (green) and post-synaptic (magenta) terminals of DNT-2A neurons seen with *DNT-2>DenMark::RFP, Dsyd1::GFP*, higher magnification in **(D),** different specimens from (B). DNT-2A projections at SMP and PRW have both pre- and post-synaptic sites. **(C)** Single neuron DNT-2A>MCFO clones. **(E)** Left: DNT-2A neurons have the vesicular glutamate transporter vGlut (arrows). Right: Colocalization between *Dop2RLex>AopCD8-GFP* and *DNT2Gal4>UASCD8-RFP* in cell bodies of DNT-2A neurons (arrows). **(F)** Terminals of dopaminergic neurons (*TH>mCD8GFP*) abut and overlap those of DNT-2A neurons (*DNT2>CD8-RFP*, magenta), arrows; magnified projections on the right. **(G)** Illustration of neurons expressing DNT-2 (magenta) and KCs, DAN PAM and PPL1, and DAL neurons **(H)** *Toll-6>FlyBow1.1* is expressed in Kenyon cells, PPL1, PPL2 and PAM DANs, as revealed by co-localization with anti-TH. **(I)** *kek-6>FlyBow1.1* co-localises with TH in MB vertical lobes, dopaminergic PALs, VUMs, PPL1, PPM2 and PPM3. SMP: superior medial protocerebrum, PRW: Prow, FLA: Flange, SOG: sub-aesophageal ganglion. Scale bars: (A-C, F-left, H, I) 50µm; (D,E,F-right) 25µm.

Figure 2 DNT-2 neurons are functionally connected to dopaminergic neurons

(A) TransTango revealed out-puts of DNT-2 neurons. All neurons express *TransTango* and expression of the TransTango ligand in DNT-2 neurons identified DNT-2 out-puts with Tomato (anti-DsRed). TransTango identified as DNT-2 outputs KC $\alpha'\beta'$ MB lobes (anterior brain, arrow, **top left**); Kenyon and possibly DAN cell bodies (posterior, arrows **top right**); DAL neurons **(bottom left,** arrows) and the dorsal layer of the fan shaped body **(bottom right,** arrow). See also Supplementary Figure S3 for further controls. **(B)** BAcTrace tests connectivity to a candidate neuron input visualised with *LexAop>sybGFP* by driving the expression of a ligand from *DNT-2GAL4* that will activate *QUASTomato* in the candidate input neuron [77]. Candidate PAM neurons visualised at SMP with GFP (green): Control: *R58E02LexA>BAcTrace 806*, no *GAL4*. Test: *R58E02LexA, DNT-2GAL4>BAcTrace 806* revealed PAMs are inputs of DNT-2A neurons at SMP (Tomato, bottom). Magenta shows QUAS-Tomato. **(C)** qRT-PCR showing that TH mRNA levels increased with DNT-2 over-expression at 30°C *(tubGAL80^{ts}, DNT-2>DNT-2FL).* One way ANOVA, P=0.0085; post-doc Dunnett's

multiple comparison test**. (D)** FRET cAMP probe Epac1 revealed that *DNT-2>Dop2R-RNAi* knockdown decreased YFP/CFP ratio over time in DNT-2A neurons, meaning that cAMP levels increased. Two-way ANOVA, genotype factor p<0.0001, time factor p<0.0001; post-doc Dunnett's. **(E,F)** Summary: DNT-2 neurons and DANs are functionally connected and modulate each other. **(E)** DNT-2 can induce *TH* expression in DANs; **(F)** this is followed by negative feedback from DANs to DNT-2 neurons. TH: tyrosine hydroxylase. Scale bars: (A) 50µm; (B) 30µm; (D) 20µm. P values over graphs in (C) refer to group analyses; stars indicate multiple comparisons tests. *p<0.05,**p<0.01, ***p<0.001. For sample sizes and further statistical details, see Supplementary Table S2.

Figure 3 DNT-2 and Toll-6 maintain PAM neuron survival in the developing and adult brain.

(A) Illustration of PAM neuronal cell bodies and experimental temporal profile. DANs are shown in green, DNT-2A neurons in magenta and MB in dark grey. The left hemisphere shows the anterior brain with PAL and PAM DAN neurons (green) and DNT-2 neurons (magenta); the right shows the posterior brain, with the calyx and other DAN neurons (PPM1, PPM2, PPM3, PPL1, PPL2, green). **(B-D)** Fruit-flies were kept constantly at 25°C, from development to adult. Analyses done in adult brains**. (B)** *DNT-2^{37}/DNT-2^{18}* mutants had fewer histone-YFP+ labelled PAM neurons (*THGAL4, R58E02-GAL4>hisYFP).* Un-paired Student t-test. **(C)** *Toll-6* RNAi knock-down in all DANs (*THGAL4, R58E02-GAL4>hisYFP, Toll-6 RNAi)* reduced Histone-YFP+ labelled PAM cell number. Un-paired Student t-test. **(D)** *DNT-2^{37}/DNT-2^{18}* mutants had fewer PAMs stained with anti-TH antibodies. Over-expressing *Toll-6^{CY}* in DANs (*THGAL4, R58E02 GAL4>hisYFP, Toll-6^{CY}*) rescued TH+ PAM neurons in *DNT-2^{37}/DNT-2^{18}* mutants, demonstrating that DNT-2 functions via Toll-6 to maintain PAM cell survival. Welch ANOVA p<0.0001, post-hoc Dunnett test. **(E-H)** Adult specific restricted over-expression or knock-down at 30°C, using the temperature sensitive GAL4 repressor *tubGAL80^{ts}*. **(E)** Adult specific *DNT-2* RNAi knockdown in DNT-2 neurons decreased Tomato+ PAM cell number (*tubGAL80^{ts}, R58E02-LexA, DNT-2 GAL4>LexAOP-Tomato, UAS DNT-2-RNAi*). Un-paired Student t-test, p= 0.005. **(F)** Adult specific *Toll-6* RNAi knock-down in *Toll-6^{31}* heterozygous mutant flies in DANs, reduced Histone-YFP+ PAM cell number (*tubGAL80^{ts}; THGAL4, R58E02-GAL4>hisYFP, Toll-6 RNAi/Toll6^{31}*). Un-paired Student t-test. **(G)**

PAMs were visualised with anti-TH. Left: *tubGAL80^{ts}, Toll-6>Toll-6-RNAi* knock-down decreased TH+ PAM cell number. Un-paired Student t-test. Right: *tubGAL80^{ts}, DNT-2>DNT-2-RNAi* knock-down decreased TH+ PAM cell number. Kruskal-Wallis ANOVA, p=0.0001, post-hoc Dunn's test. **(H)** Adult-specific *tubGAL80^{ts}, DNT-2>DNT-2RNAi* knock-down increased the number of apoptotic cells in the brain labelled with anti-DCP-1. Dcp-1+ cells co-localise with anti-TH at least in PAM clusters. One Way ANOVA, p<0.0001, post-doc Bonferroni's multiple comparisons test. DANs>histone-YFP: all dopaminergic neurons expressing histone-YFP, genotype: *THGal4 R58E02Gal4>UAS-histoneYFP*. *PAMsLexA>tomato*: restricted to PAM DANs: *R58E02LexA>LexAop-nlstdTomato.* Controls: *GAL4* drivers crossed to wild-type Canton-S. Scale bars: (B-G) 30µm; (H) 20µm. Graphs show box-plots around the median. P values over graphs in (D, G right, H) refer to group analyses; stars indicate multiple comparisons tests. *p<0.05, **p<0.01, ***p<0.001. For further genotypes, sample sizes and statistical details, see Supplementary Table S2.

Figure 4 DNT-2, Toll-6 and Kek-6 are required for arborisations and synapse formation. (A) Illustration showing the ROIs (dashed lines) used for the analyses, corresponding to dendrites and axonal endings of PAMs and axonal terminals of PPL1ped neurons. **(B-F)** Fruit-flies were kept constantly at 25°C. **(B)** Complete loss of PAM synapses (*PAM>syt-GFP*) onto α,β MB lobe in *DNT-2* null mutants. **(C)** *Toll-6* RNAi knockdown in PAM β2β'2 neurons (*MB301B>FB1.1, Toll-6-RNAi*) decreased dendrite complexity. Un-paired Student t-test. **(D)** Over-expression of cleaved *DNT-2CK* in PAM β2β'2 neurons *(MB301B>CD8-GFP, DNT-2CK)* increased dendrite complexity. Un-paired Student t-test. **(E,E',F)** PPL1ped axonal misrouting was visualised with *split-GAL4 MB320CGal4>FlyBow1.1.* Images show PPL1-γped neurons and some PPL1-α2α'2. **(D,D')** RNAi knock-down of *Toll-6, kek-6* or both (e.g. *MB320CGal4>FlyBow1.1, Toll-6RNAi)* in PPL1-γped neurons caused axonal terminal misrouting (arrows). **(E')** Higher magnification of **(E,** dotted squares**)**. Chi-square for group analysis: p = 0.0224, and multiple comparisons Bonferroni correction control vs *Toll-6RNAi* p<0.01; vs *kek-6RNAi* p<0.05; vs *Toll-6RNAi kek-6RNAi* p<0.01, see Table S2**. (F)** PPL1 misrouting was also induced by over-expressed *DNT-2CK* or *DNT-2FL* (e.g. *MB320CGal4>FlyBow1.1, DNT-2FL)*. Chi-square for group analysis: p<0.05, Bonferroni correction control vs *DNT-2CK* ns, vs *DNT-2FL* *p<0.05, see Table S2.

(G) Adult-specific *Toll-6 kek-6 RNAi* knockdown in PAM neurons decreased size of post-synaptic density sites (*PAM>Homer-GCaMP* and anti-GFP antibodies). Temperature regime shown on the right. **(C,D)** Graphs show box-plots around the median; **(G)** are box-plots with dot plots. (C,D,G) *p<0.05, **p<0.01, ****p<0.0001. Scale bars: (B,C,D,E) 30µm; (E',F,G) 20µm. For genotypes, sample sizes and statistical details, see Supplementary Table S2.

Figure 5 DNT-2 neuron activation and DNT-2 over-expression induced synaptogenesis. (A) Thermo-activation of DNT-2 neurons at 30°C altered DNT-2 arborisations, here showing an example with smaller dendrites and enlarged axonal arbours (magenta shows 3D-rendering of axonal arborisation done with Imaris, merged with raw image in green). (Genotype: *DNT-2>FlyBow1.1, TrpA1*). **(B)** Thermogenetic activation of DNT-2 neurons increased the number of Homer+ PSDs in DNT-2 neurons, at SMP (*DNT-2>Homer-GCAMP3, TrpA1*, anti-GFP). Test at 30°C 24h: Unpaired Student t test. See Table S2. **(C)** Thermogenetic activation of DNT-2 neurons induced synaptogenesis in PAM target neurons at SMP, but not at MB lobe. (Genotype: *PAM(R58E02)LexA/LexAOP-sytGCaMP; DNT-2GAL4/UASTrpA1*). At SMP: No. Syt+ synapses: Mann Whitney-U; Syt+ synapse volume: Mann Whitney-U. At MB lobe: No. Syt+ synapses: Unpaired Student t ns; Syt+ synapse volume: Mann Whitney-U ns. **(D)** Over-expression of DNT-2FL in DNT-2 neurons increased synapse volume at SMP dendrite and induced synaptogenesis at MB lobe. (Genotype: *PAM(R58E02)LexA/LexAopSytGcaMP6; DNT-2Gal4/UAS-DNT-2FL*). At SMP: No. Syt+ synapses: Unpaired Student t ns. Syt+ synapse volume: Mann Whitney-U. At MB lobe: No. Syt+ synapses: Unpaired Student t; Syt+ synapse volume: Mann Whitney-U ns. Graphs show box-plots around the median, except for PSD volume data that are dot plots. *p<0.05, ****p<0.0001; ns: not significantly different from control. Scale bars: 30µm. For Genotypes, sample sizes, p values and other statistical details, see Supplementary Table S2.

Figure 6 DNT-2-induced circuit plasticity modified dopamine-dependent behaviour. (A) *DNT-2* mutants (left, *DNT-2*^{37}*/DNT-2*^{18}) and flies with adult-specific RNAi knock-down of *DNT-2* in DNT-2 neurons (right, *tubGAL80*^{ts}*; DNT-2>DNT-2RNAi*), had impaired climbing. Left Mann Whitney U; Right: One Way

ANOV, post-hoc Dunnett. **(B)** Adult-specific *Toll-6* and *kek-6* RNAi knock-down in Toll-6 *(tubGAL80^{ts}; Toll-6>Toll-6RNAi, kek-6RNAi,* left) or PAM (*tubGAL80^{ts}; R58E02>Toll-6RNAi, kek-6RNAi,* right) neurons impaired climbing. Left: Welch ANOVA, post-hoc Dunnett. Right: Welch ANOVA, post-hoc Dunnett. **(C)** The climbing impairment of *DNT-2* mutants could be rescued with the over-expression of *Toll-6^{CY}* in dopaminergic neurons (Rescue genotype: UASToll-6^{CY}/+; DNT-2^{18}*THGAL4 R58E02GAL4/DNT-2^{37}).* Welch ANOVA, post-hoc Dunnett. **(D)** Adult specific over-expression of *Toll-6^{CY}* in DANs increased locomotion in *DNT-2^{37}/DNT-2^{18}* mutants. (Test genotype: *UASToll-6^{CY}/+; DNT-2^{18}THGAL4 R58E02GAL4/DNT-2^{37}*). Walking speed: Kruskal Wallis ANOVA, post-hoc Dunn's. Distance walked: Kruskal Wallis ANOVA, post-hoc Dunn's. Time spent immobile: Kruskal Wallis ANOVA, post-hoc Dunn's. **(E)** Adult specific *DNT-2FL* overexpression in DNT-2 neurons increased fruit-fly locomotion speed in an open arena at 30°C (see also Supplementary Figure S6A for further controls). (Test genotype: *tubGAL80^{ts}, DNT-2>DNT-2FL*) Kruskal-Wallis, post-hoc Dunn's test. **(F)** Thermogenetic activation of DNT-2 neurons at 30°C *(DNT-2>TrpA1)* increased fruit-fly locomotion speed. (See also Supplementary Figure S6B for further controls). One Way ANOVA p<0.0001, post-hoc Dunnett's test**. (G)** Over-expression of *DNT-2-FL* in DNT-2 neurons increased long-term memory. (Test genotype: *tubGAL80^{ts}, DNT-2>DNT-2FL*). Left: 23°C controls: One Way ANOVA p=0.8006. Right 30°C: One Way ANOVA, post-hoc Dunnett's test. Graphs show box-plots around the median, under also dot plots. P values over graphs refer to group analyses; asterisks indicate multiple comparisons tests. *p<0.05, **p<0.01, ***p<0.001, ****p<0.0001; ns: not significantly different from control. For further genotypes, sample sizes, p values and other statistical details, see Supplementary Table S2.

SUPPLEMENTAL INFORMATION

Supplementary Figure S1 Identification of neurotransmitter type for DNT-2A neurons. (A, B) Anterior DNT-2A neurons projecting at SMP are not dopaminergic, as there was no co-localisation between *DNT-2>histoneYFP* and anti-TH in the anterior brain **(A),** and there was no colocalization in other DNT-2+ neurons in the posterior brain either **(B).** Higher magnification of dotted boxes on the right. **(C)** There was no colocalisation with *Dop1R2LexA>CD8::GFP, DNT-2Gal4>CD8::RFP* either. **(D)** DNT-2 neurons are not not

serotonergic, as there was no co-localization between *DNT-2>FlyBow1.1* and the serotoninergic neuron marker anti-5HT**. (E)** There are not octopaminergic, as there was no overlap between *TdcLexA>mCD8::GFP and DNT-2Gal4>CD8::RFP*. **(F)** There was no overlap between *DNT-2Gal4>histoneYFP* and the cholinergic neuron marker anti-ChAT4b1. **(G,H)** Anterior DNT-2A neurons are not GABAergic, but lateral DNT-2 neurons are, as visualised with *DNT-2>CD8-RFP, GADLexA>CD8-GFP*. Scale bars: (A,B left) 50µm; (C-H) 20 µm. For further genotypes and sample sizes, see Supplementary Table S2.

Supplementary Figure S2 Identification of *Toll-6* and *kek-6* expressing neurons. (A) *Toll-6Gal4, MB247-Gal80>UASFlyBow1.1* and *kek-6Gal4, MB247-Gal80>UASFlyBow1.1* revealed Toll-6+ and Kek-6+ projections on MB g2a'1. **(B)** *R25D01LexA>CD8GFP, kek6-Gal4>CD8RFP* overlapped in MB g2a'1. **(C)** *R14C08LexA>CD8GFP, Toll-6Gal4>CD8-RFP13* revealed co-localization in MBON-M4/M6 cell bodies. **(D,E)** Co-localisation of *Toll-6>Histone-YFP* and *kek-6>HistoneYFP* with TH in PPL1 neurons. **(F)** Number of PAM and PPL1 neurons expressing *Tolls* and *kek-6,* revealed from published RNAseq data (Scope, see also Table S1). **(G, H)** Toll-6 and kek-6 are expressed in DAL neurons. **(G)** DAL neurons express *Toll-6,* as revealed by co-localization between *DAL-LexA (VT49239-LexA)>mCD8-GFP* and *Toll-6GAL4>mCD8-RFP*. **(H)** DAL neurons express *kek-6*, as revealed by colocalization between *DAL-LexA (VT49239-LexA)>mCD8-GFP* and *kek6GAL4>mCD8RFP*. **(I, J)** Toll-6 and kek-6 are expressed in MB neurons. **(I)** *Toll-6>MCFO* clones reveal expression at least in MB neurons g medial (gm), abcore (abc) and absurface (abs). **(K)** *kek-6>MCFO* clones reveal expression at least in MB Kenyon cells aba'b'g formed and MB g2a'1 and a2a'2 and PPL1-$\gamma 2\alpha'1$ and PPL1-$\alpha 2\alpha'2$. Scale bars: (B, H) 50µm; (A,C,D,G, I, J) 30µm. For further genotypes and sample sizes, see Supplementary Table S2.

Supplementary Figure S3 TransTango connectivity controls. (A) *UAS-TransTango/+* control, showing background GFP expression in mushroom bodies and Tomato+ signal in sub-aesophageal ganglion (SOG). **(B)** *DNT-2GAL4>UAS-TransTango*, revealing the GFP+ DNT-2 neurons and Tomato+ signal in DNT-2 neurons. TransTango also reveals what appears to be feedback connections between DNT-2 neurons from SMP to

PRW (arrow). These are controls for Figure 3A. Scale bars: (A,B) 50µm. For further genotypes and sample sizes, see Supplementary Table S2.

Supplementary Figure S4 Neuronal activity increased production and cleavage of DNT-2. (A) Thermogenetic activation of DNT-2 neurons increased the number of DNT-2FLGFP+ vesicles or spots (*DNT-2>DNT-2-FL-GFP*, *TrpA1* with anti-GFP). Control 18°C: Unpaired Student t test, ns. Activation 30°C 24h: Mann Whitney**. (B)** Western blot from fly heads over-expressing DNT-2FL-GFP in DNT-2 neurons showing that neuronal activation with TrpA1 at 30°C increased DNT-2FL-GFP cleavage. **(**Genotype: *DNT-2>TrpA1, DNT-2FL-GFP*). Controls are flies of the same genotype kept constantly at 18°C as well as flies treated also at 30°C but lacking TrpA1. High temperature (30°C) is sufficient to increase fly activity. ***p<0.001. ns= not significant. For further genotypes, sample sizes, p values and other statistical details see Supplementary Table S2.

Supplementary Figure S5 Controls for Figure 5B. Control at 18°C, for Figure 5B. DNT-2 bidirectional arborisation at SMP was visualised with Homer-GCaMP and anti-GFP antibodies (*DNT-21>homer-GCAMP* and *DNT-2>homer-GCAMP, TrpA1* at 18°C). Unpaired Student t-test, ns. Scale bars: (A,B) 30µm. For further genotypes, sample sizes, p values and other statistical details see Supplementary Table S2.

Supplementary Figure S6 Locomotion in open arena controls. (A) Controls for Figure 6E. In 18°C controls, GAL80 is on and GAL4 is off, thus there is no adult specific *DNT-2FL* overexpression in DNT-2 neurons in these flies. (Genotype: *tubGAL80ts, DNT-2>DNT-2FL*). Consistently, there was no increase in locomotion speed in an open arena, in flies over-expressing *DNT-2FL* relative to controls, compare also to Figure 6E. Kruskal Wallis ANOVA ns (lower median in *UAS-DNT-2FL/+* control). **(B)** Controls for Figure 6F. The cation TrpA1 opens at high temperatures (eg 30°C) but remains closed at 18°C. Consistently, there was no effect in locomotion at 18°C in flies of genotype *DNT-2>TrpA1* compared to controls, compare also to

30°C data in Figure 6F. Kruskal Wallis ANOVA ns. For further genotypes, sample sizes, p values and other statistical details see Supplementary Table S2.

Supplementary Figure S7 **Altering *DNT-2* levels induced seizures.** Knock-down or over-expression of *DNT-2* in the adult, using *GAL80*^{ts}. Fruit-flies were reared at 18°C from egg laying to adult eclosion, when they were transferred to 30°C and kept there for 5 days prior to testing**.** To test for seizures, we used the bang-sensitivity test. *DNT2*^{37}*/DNT2*^{18} mutant flies (left) and adult *DNT-2* knock-down flies (*tubGal80*^{ts} *DNT-2Gal4>DNT-2RNAi,* centre) took longer to recover than controls. Over-expression of *DNT-2FL* in DNT-2 neurons (*tubGal80*^{ts} *DNT-2Gal4>DNT-2FL,* right) increased variability in recovery time. For further genotypes and sample sizes see Supplementary Table S2.

Table S1 **Expression of *Tolls, keks* and Toll downstream adaptors in cells related to DNT-2A neurons.** Genes expressed in DNT-2 neurons, their potential and/or experimentally verified inputs and outputs, were identified with a combination of reporters (this work) and data from public single-cell RNAseq databases.

Table S2 **Statistical analysis.** Table providing full genotypes, sample sizes, statistical tests, multiple comparison corrections and p values.

FIGURE 1 Neurons expressing *DNT-2* and its receptors *Toll-6* and *kek-6* in the adult brain

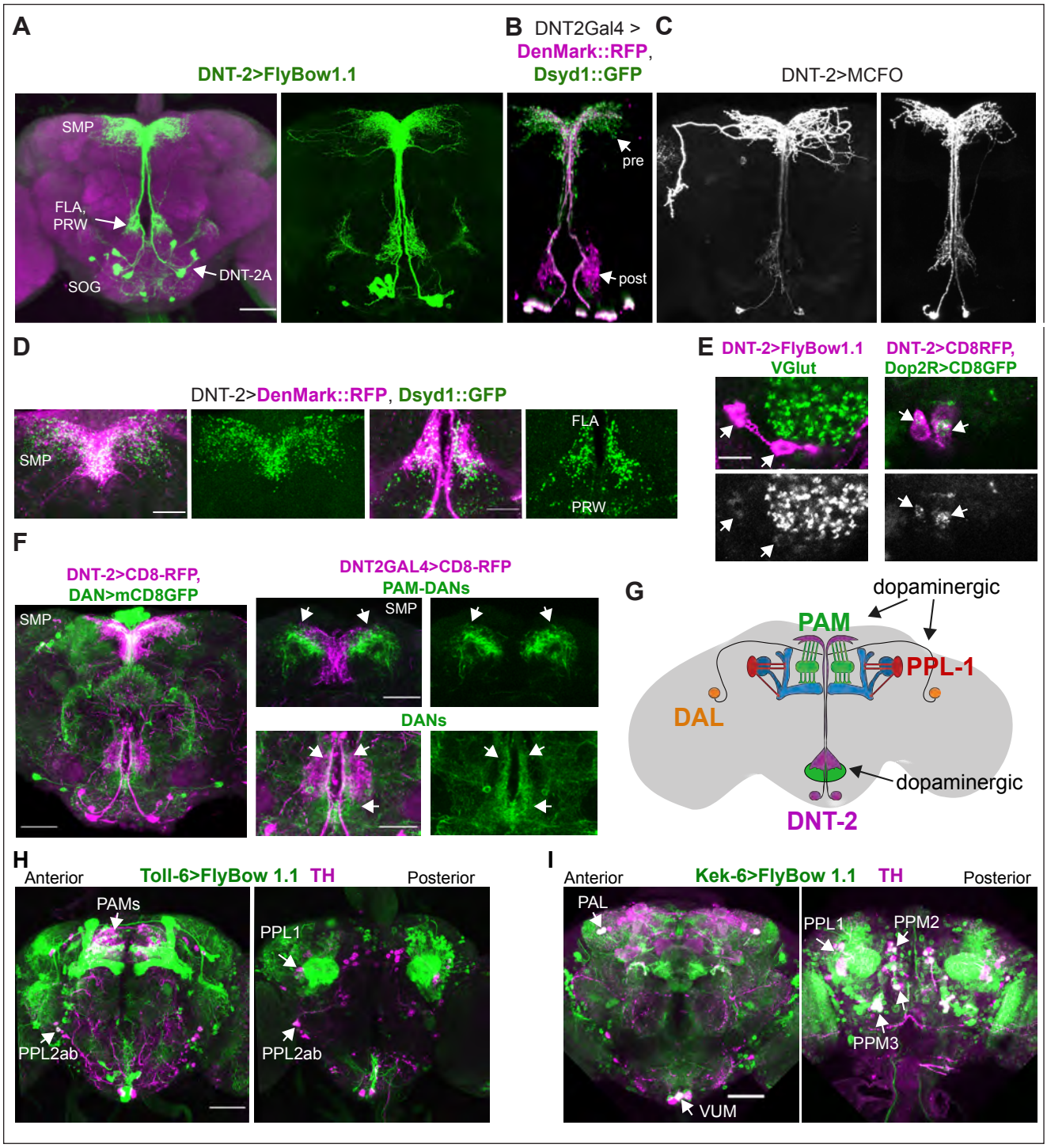

Figure 2 DNT-2 neurons are functionally connected to dopaminergic neurons

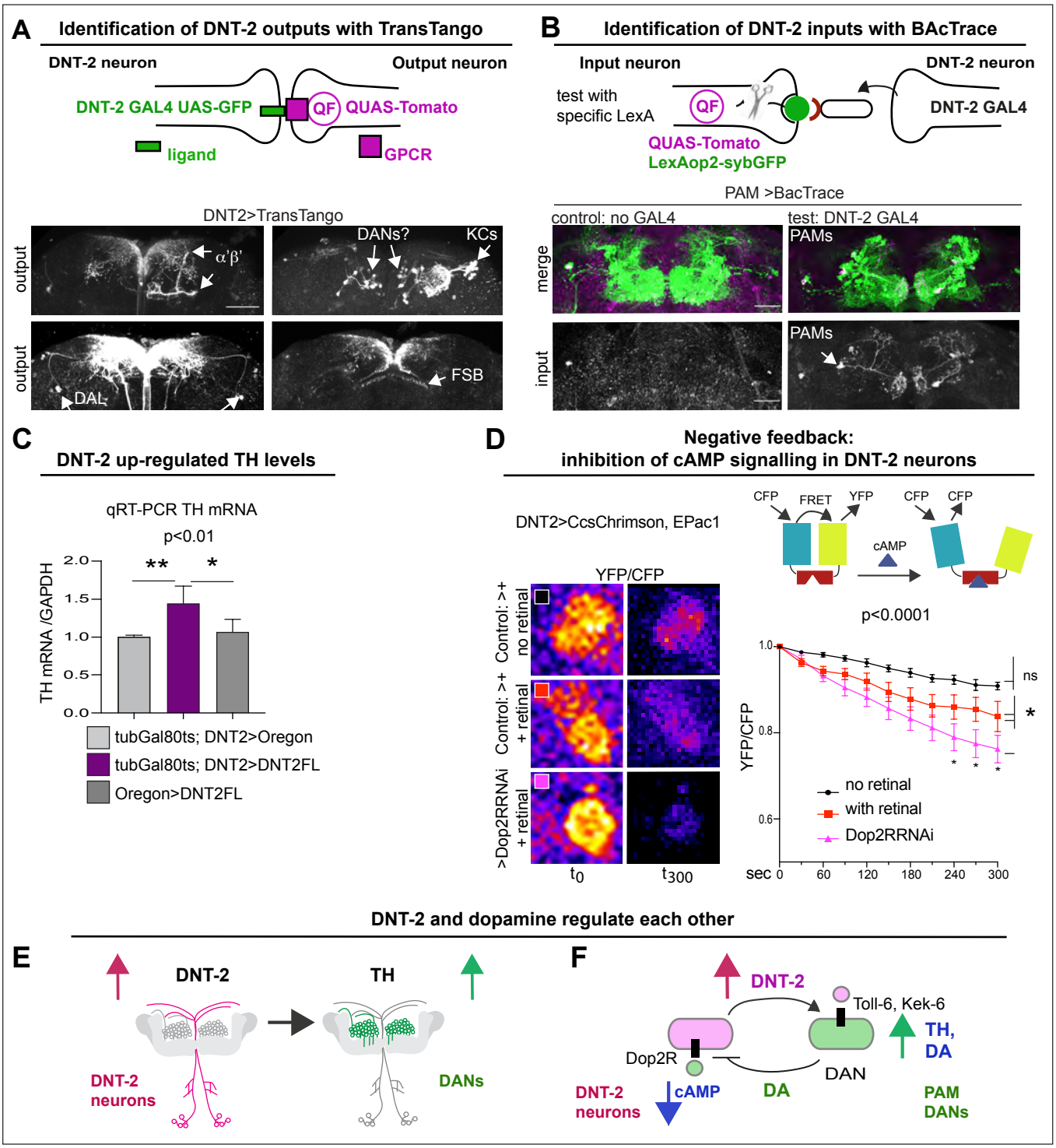

Figure 3 DNT-2 and Toll-6 maintain PAM neuron survival in the developing and adult brain

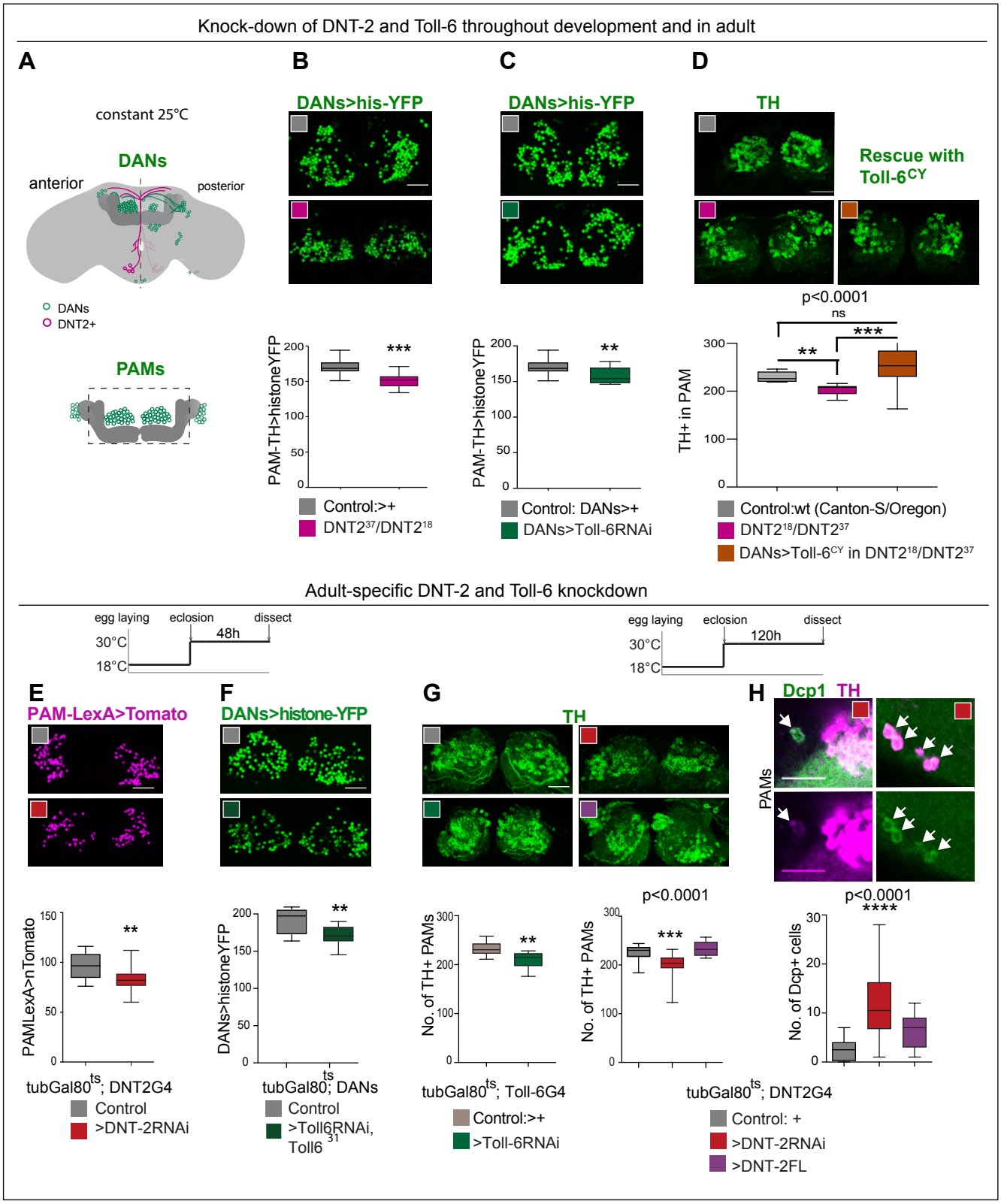

Figure 4 DNT-2, Toll-6 and Kek-6 are required for synapse formation and arborisations

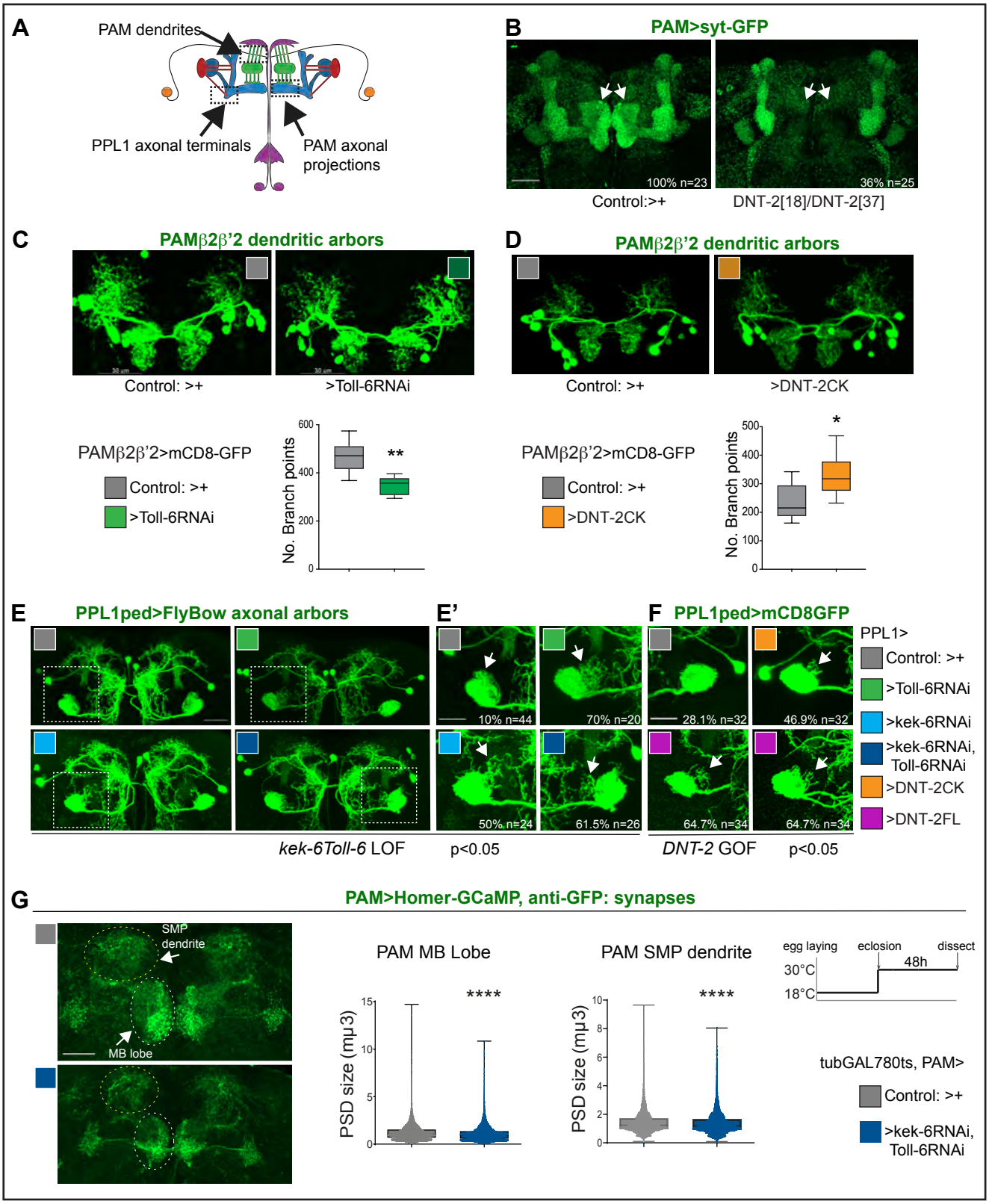

Figure 5 DNT-2 neuron activation and DNT-2 over-expression induce synaptogenesis

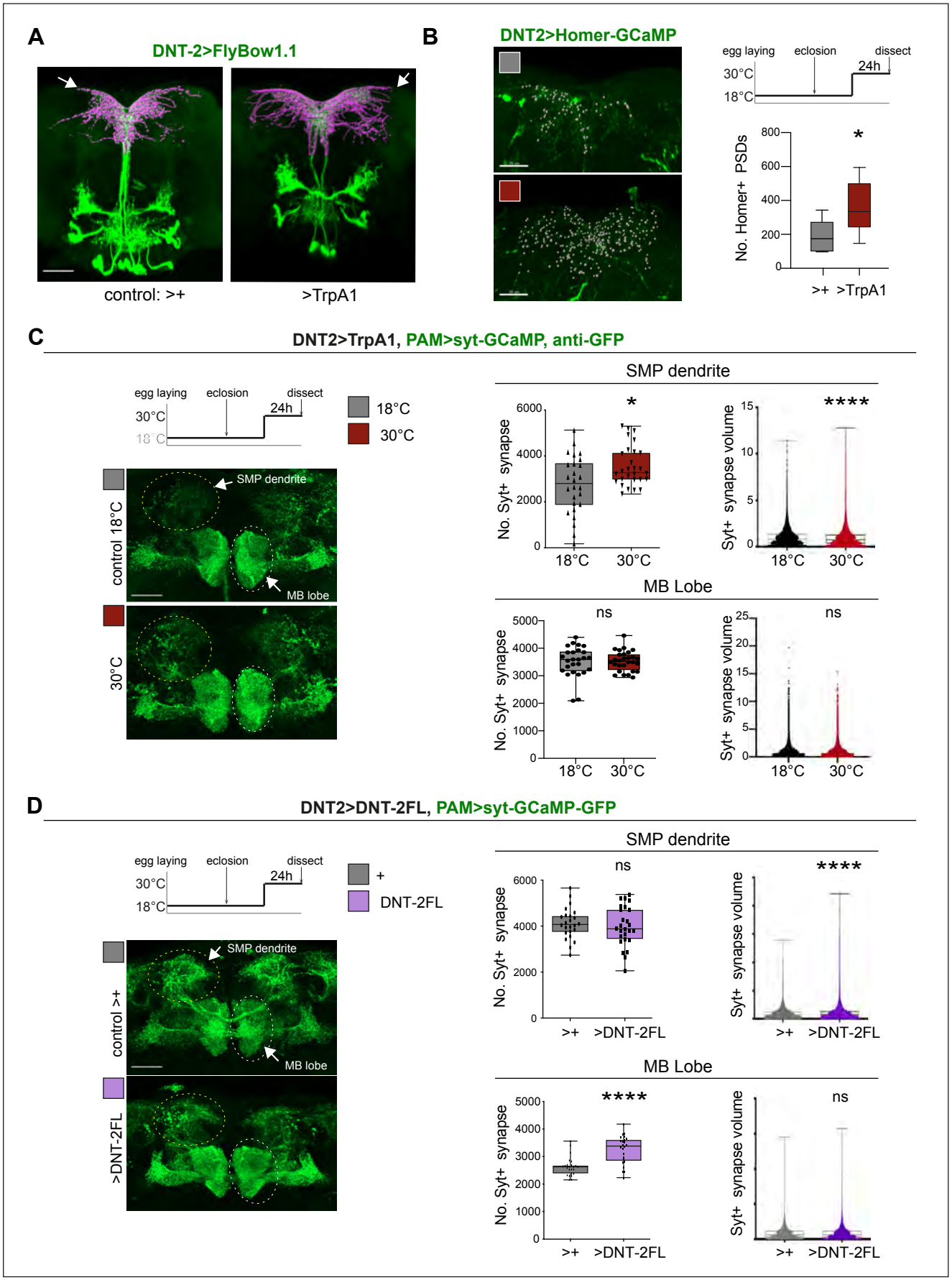
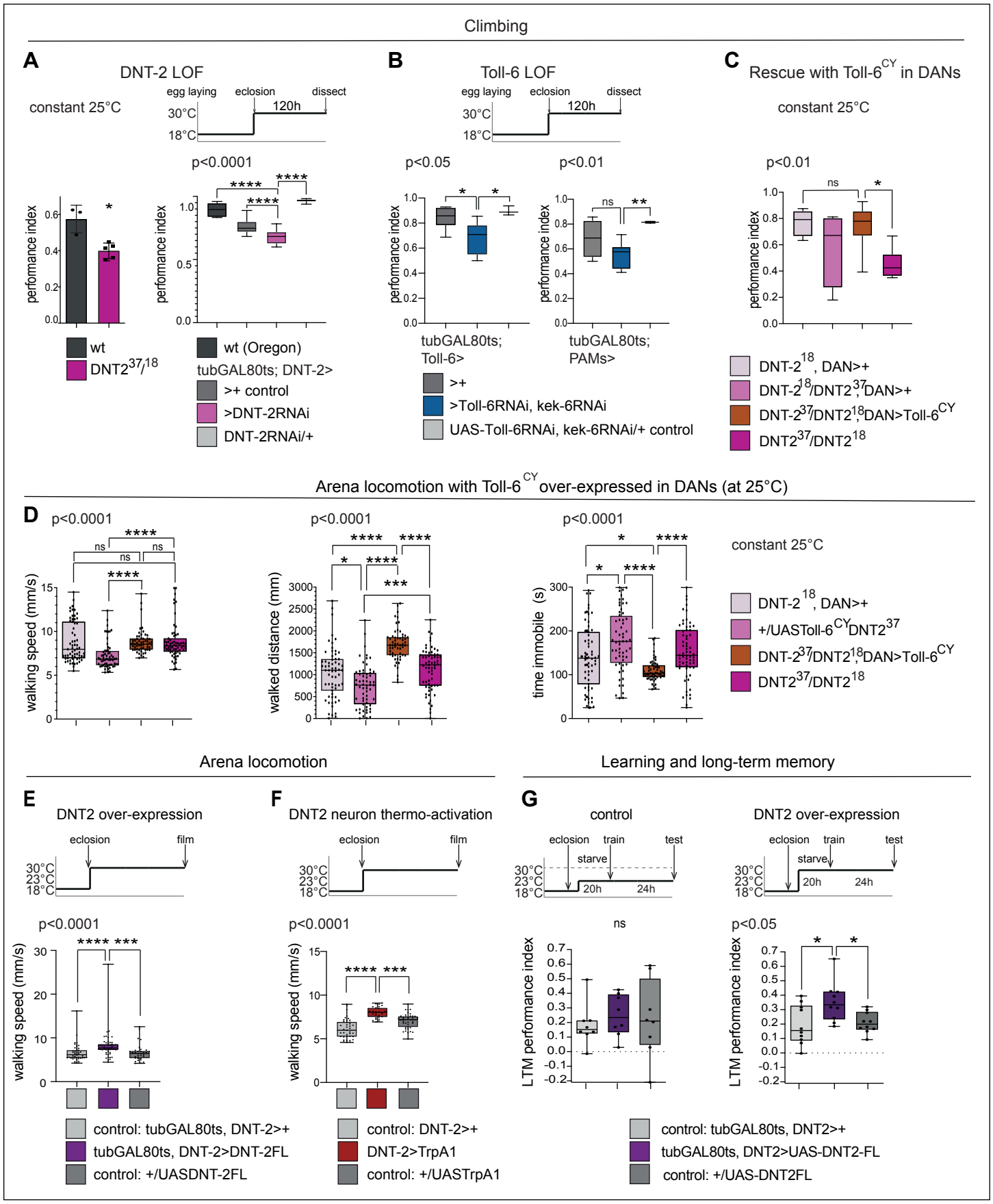
Figure 6 DNT-2-induced circuit plasticity modified dopamine-dependent behaviours.